



WPI

OPTIMAL DRIVELINE ROBOT BASE

Development of a driveline with low speed
maneuverability and high speed stability

Submitted in partial fulfillment of the Bachelor of Science degree of
Worcester Polytechnic Institute, Worcester, MA

Submitted to:

Prof Kenneth Stafford (advisor)

Prof Taskin Padir (co-advisor)

Michael Cullen (ME)

Stephen Diamond (RBE/ECE)

William Dunn (RBE)

Kirk Gimsley (RBE)

Submitted on: May 1st, 2014

Advisor Signature

Co-advisor Signature

Authorship

The Background and Design Goals were written by all group members collaboratively. The other sections of this report were primarily written by individual members as specified below.

Name	Contributions
Michael Cullen	Manufacturing- Steering Assembly, Design-Steering Assembly, Testing & Evaluation, Results
Stephen Diamond	Design- Electrical and Programming, Budget, Schematic, Manufacturing- Programming Implementation
William Dunn	Manufacturing- Chassis, Manufacturing- Wheel Modules, Design- Chassis, Design- Wheel Modules, Social Implications, Discussion, Results
Kirk Grimsley	Manufacturing- Electrical Systems, Manufacturing- Programming, Executive Summary, Design Selection, Discussion, Final Conclusions

Abstract

Our team has decided that there is currently a need for a driveline system that is capable of performing a zero radius turn and being maneuverable at low speeds while also maintaining traction, stability, and energy efficiency at high speeds. We designed and prototyped a modified Ackermann steering system driven by a single motor, with an extended range of motion. This driveline system also enforces that all wheels are driven in all conditions. The steering system was integrated into a robot chassis that meets FRC requirements.

Table of Contents

AUTHORSHIP	1
ABSTRACT	2
TABLE OF FIGURES	5
EXECUTIVE SUMMARY	6
BACKGROUND	8
EXISTING DRIVE SYSTEMS	8
<i>Ackermann Steering</i>	8
<i>Holonomic Drive</i>	9
<i>Swerve Drive</i>	11
<i>Tank Drive</i>	12
<i>Chassis Steering</i>	13
FIRST ROBOTICS	14
<i>FIRST Constraints</i>	14
<i>Team 190 Survey</i>	15
<i>Past FRC Designs</i>	15
DESIGN GOALS	18
PRIMARY GOALS	18
<i>High-Speed Stability</i>	18
<i>Low-Speed Maneuverability</i>	18
GENERAL GOALS	18
PROJECT DESIGN	20
DESIGN SELECTION	20
MECHANICAL SYSTEMS	23
<i>Steering Assembly</i>	23
<i>Wheel Modules</i>	29
<i>Chassis</i>	36
ELECTRICAL SYSTEMS	38
<i>Motor Selections</i>	38
<i>Sensors</i>	40
<i>Teleoperation</i>	41
<i>Schematic</i>	41
PROGRAMMING	42
<i>Motor Control</i>	42
<i>Pseudo code</i>	43
BUDGET	44
MANUFACTURING AND ASSEMBLY	46
MECHANICAL SYSTEMS	46
<i>Chassis</i>	46
<i>Front Wheel Modules</i>	48

<i>Rear Wheel Modules</i>	50
<i>Steering Assembly</i>	51
ELECTRICAL ASSEMBLY	55
PROGRAMMING IMPLEMENTATION.....	57
TESTING AND EVALUATION	60
INDIVIDUAL PERFORMANCE EVALUATION.....	60
COMPARATIVE PERFORMANCE EVALUATION.....	60
CONCLUSION	62
RESULTS	62
DISCUSSION	63
SOCIAL IMPLICATIONS	65
FINAL CONCLUSIONS.....	66
APPENDICES	67
APPENDIX A: DRIVER PERFORMANCE COURSE DATA	67
APPENDIX B: CODE.....	67
APPENDIX C: FRC MOTOR DATA	77
APPENDIX D: POWER REQUIREMENT DATA	77
APPENDIX E: BOSCH VAN DOOR MOTOR OUTPUT DATA	78

Table of Figures

FIGURE 1: ACKERMANN STEERING.....	9
FIGURE 2: MECANUM WHEEL.....	10
FIGURE 3: MECANUM DRIVE	10
FIGURE 4: SWERVE DRIVE FRAME	11
FIGURE 5: SWERVE DRIVE - CLOSE-UP CONFIGURATION	12
FIGURE 6: TRADITIONAL ZERO-TURN LAWNMOWER.....	13
FIGURE 7: 2013 "ULTIMATE FUNKY OBJECT" BY LYNBROOK ROBOTICS	15
FIGURE 8: ROBOWRANGLERS 2008 FRC ROBOT, "TUMBLEWEED"	16
FIGURE 9: CONCEPTUAL AMPLIFIED ACKERMANN STEERING.....	24
FIGURE 10: ZERO RADIUS TURNING CONDITIONS.....	24
FIGURE 11: TRAPEZOIDAL STEERING GEOMETRY	25
FIGURE 12: DESIGNED VERSUS PERFECT ACKERMANN PLOT	27
FIGURE 13: CONCEPTUAL STEERING ARM DESIGN.....	27
FIGURE 14: STEERING ARM RANGE OF MOTION	28
FIGURE 15: REQUIRED STEERING ARM POWER.....	29
FIGURE 16: ANDYMARK WILD SWERVE DRIVE MODULE.....	31
FIGURE 17: ORIGINAL BRACKET ASSEMBLY	32
FIGURE 18: MODIFIED BRACKET ASSEMBLY	32
FIGURE 19: PARTIAL KIT FOR REAR WHEELS	33
FIGURE 20: FINAL MODIFIED WILD SWERVE MODULE FOR FRONT WHEELS	34
FIGURE 21: NEW 22 TOOTH SPROCKET WITH HOLES DRILLED	34
FIGURE 22: MODIFIED SPROCKET ASSEMBLY.....	35
FIGURE 23: PART DRAWING FOR REAR WHEEL MODULE PLATE.....	35
FIGURE 24: OFF-THE-SHELF VEX CHASSIS.....	36
FIGURE 25: CHASSIS DESIGN WITH VEX ANGLE BARS	37
FIGURE 26: FINAL CAD MODEL	38
FIGURE 27: VAN DOOR MOTOR OUTPUT TORQUE	40
FIGURE 28: ELECTRICAL SCHEMATIC.....	42
FIGURE 29: LIST OF EXPENSES	45
FIGURE 30: PARTIAL FRAME DURING ASSEMBLY	47
FIGURE 31: COMPLETED FRAME WITH WHEEL MODULES.....	47
FIGURE 32: SPROCKET ASSEMBLY COMPONENTS.....	48
FIGURE 33: MODIFIED SPROCKET ASSEMBLY	49
FIGURE 34: COMPLETED ASSEMBLY IN PLACE	50
FIGURE 35: CAD FOR WHEEL SHAFT	51
FIGURE 36: COMPLETED REAR WHEEL ASSEMBLY	51
FIGURE 37: TIE ROD (TOP) AND STEERING ARM (BOTTOM).....	52
FIGURE 38: PLATE SPROCKETS WITH SLOTS (LEFT) AND TIE ROD/SPROCKET ASSEMBLY (RIGHT).....	53
FIGURE 39: MANUFACTURED STEERING ASSEMBLY WITH STANDOFFS.....	53
FIGURE 40: NEW STEERING ARM ASSEMBLY.....	54
FIGURE 41: COMPLETED ROBOT DRIVELINE AND CHASSIS	54
FIGURE 42: A PICTURE OF OUR POTENTIOMETER WITH THE 3D PRINTED ADAPTER TO THE TURNING MOTOR.	57
FIGURE 43: WHEEL VELOCITY VS. STEER ANGLE	59
FIGURE 44: PERFORMANCE COURSE	61
FIGURE 45: AVERAGE DRIVER COURSE TIMES	63

Executive Summary

Our team has analyzed different frequently used drivelines and determined that they all have distinct weaknesses that we could improve upon. The most commonly used driveline on a robotic chassis, especially for FIRST Robots, which we will be what we compare our system to, is tank drive. This style of driving has two significant drawbacks: an inability to handle well at high speed, and, since it turns via skid steer, it is very energy inefficient. Another is swerve drive, which is extremely maneuverable and can be programmed so that it handles well, but takes a significant number of motors, a lot of programming and a high level of user skill to operate well. The type of steering most people will be familiar with is Ackermann steering, which is what a traditional car uses. The issue with a car is that even though it handles extremely well at high speeds, at lower speeds it requires significant effort to make precise, small radius turns.

Based on this analysis we set about creating a system that would be able to maintain high speed handling, low speed maneuverability, and maximize energy efficiency by reducing wheel skid. To do this we evaluated different options for drivelines and determined that the one that best met our requirements was an “Enhanced Ackermann” system. This system would use a standard car Ackermann, but we would modify the wheels and the tie rod linkage so that they would turn 147° instead of the approximately 60° a normal car can turn. This allows us to reduce the radius of the circle the driveline is turning about, until it is turning about one of the back wheels. Therefore, when making a left hand turn, our chassis pivots about the back left wheel and when making a right hand turn, it pivots about the right rear wheel. In order to do this we had to use specific geometry to make sure the wheel angles changed at the proper ratios to one another, as well as create wheel speed algorithms to determine how fast each individual wheel should be spinning depending on how tight any given turn is.

Once we implemented our system we were able to drive it through a course and compare the number of obstacles hit, and time to run the course. We also evaluated a typical skid-steered FRC robot with the same drivers. During this testing our robot was slightly slower than the FRC robot and it also hit more obstacles. However, upon discussing the results of the driving with the participants we found that they were all extremely happy with the handling and mechanical systems of our driveline. Instead, we found that they felt the majority of the reason for the setbacks was the remote control system being used. We had opted for an RC airplane style controller, and most felt the range of motion available to the joysticks was too small to

allow for easy handling of our system. Based on this feedback and the results we saw, we feel that mechanically our chassis was able to meet all of the requirements, but that the user interface needed additional time to properly implement and optimize for our system. Of the initial goals we set out to achieve, the only one we failed to meet was to complete the course faster than a traditional FRC robot. We were able to accomplish the goals of reaching a speed of at least 10 ft/sec, maintaining a 4 foot lane while driving a 10 foot radius circle, being able to turn about a point within the perimeter of the chassis, maximizing for traction at lower speeds by driving all wheels, maximizing energy efficiency by minimizing skidding, and complying with all rules and requirements from the FRC 2013 season.

Background

Existing Drive Systems

Ackermann Steering

Ackermann steering is based on the fact that when a vehicle goes around a turn, the wheels on the outside have to travel farther, and they follow a different arc than the wheels on the inside of the turn. Modern cars do not use a pure Ackermann steering due to some limitations in high-speed maneuvers. Race cars use a reverse Ackermann steering which is better for high speed maneuvers.

During traditional Ackermann steering, each of the four wheels must spin at a different speed to prevent skidding. The front tires tend to spin at a faster rate than the rear tires, and the wheels on the outside of the turn must rotate faster than the inside wheels. So for a left turn, the right-front tire spins the fastest out of the four while the left rear tire spins the slowest.

This is accomplished by differentials and different turning angles for each front wheel. Since the axes of all four wheels must be oriented toward the point about which the vehicle is turning, the two front tires pivot at different angles for any given turn while the rear wheels remain fixed to their shared axle. For a left turn, the left front wheel is turned at a different angle than the right front wheel because of the different arc that each wheel needs to make in order to prevent tire slip.

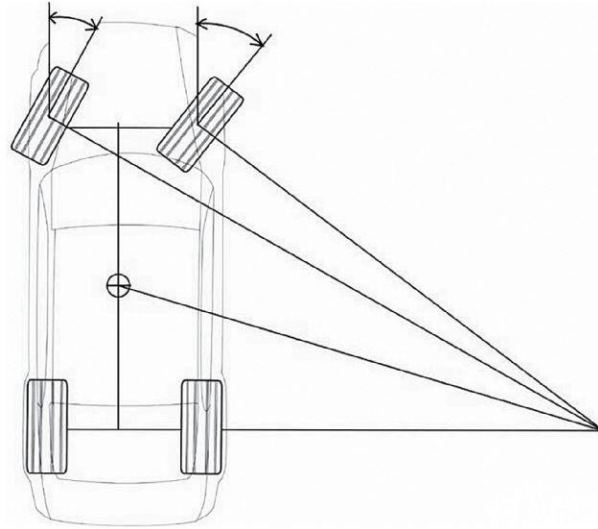


Figure 1: Ackermann Steering

Triple Differential

A triple differential is needed in order for Ackermann steering to function with all-wheel drive (AWD) systems. Without a triple differential, problems can occur due to transmission wind up or lock up due to the tires not being able to spin at different speeds around corners.

A triple differential is setup with a differential on both the front and rear axles and an additional differential on the drive shaft coming from the transmission or transfer case. The differentials on the axles allow the wheels to spin at different speeds around corners, which prevents tire slip. However, a center differential is also required to allow the front axle to travel further than the rear axle to prevent transmission lock up around corners.

Holonomic Drive

The holonomic drive system uses multiple specialized wheels such that the robot can move in any direction by running the wheels at different speeds. This provides a high degree of maneuverability because the robot does not have to rotate its chassis or wheel modules before moving in any given direction. Any direction of motion can be achieved simply by driving each wheel at the correct speed. This requires the wheels to be able to slide laterally, so omni or mecanum wheels are generally used.



Figure 2: Mecanum wheel

This drive system is not always intuitive, and controlling each wheel directly is difficult for an operator. To make this easier to control, it is helpful to implement a solution on the firmware level that uses the desired direction of motion to calculate the required speeds of each wheel. This allows a holonomic drive robot to be controlled more easily.

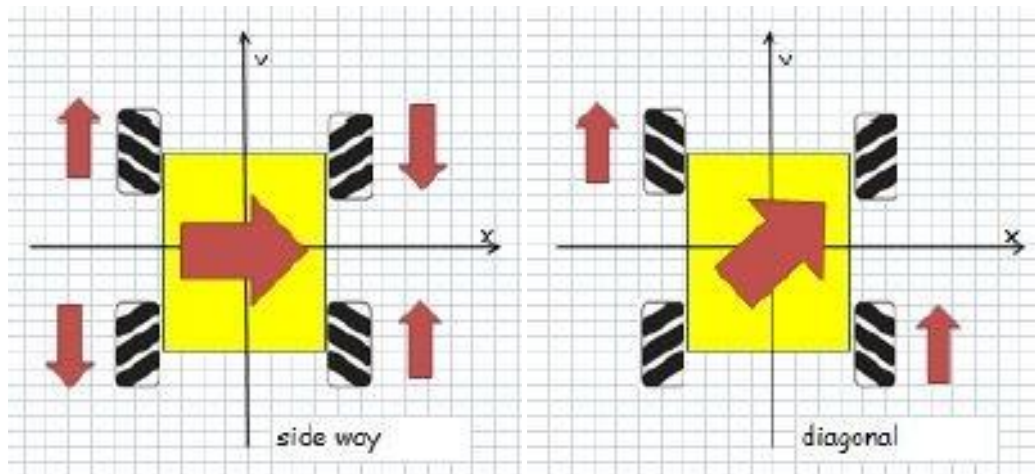


Figure 3: Mecanum Drive

Mecanum-wheeled, holonomic drive robots are common due to the fact that they are mechanically simple and extremely maneuverable at low speeds. The ability to achieve rotation (zero turn radius) or translation in any direction immediately (without first having to turn the

robot) makes it very advantageous. The down side is that this system is relatively complex from a control standpoint. Determining how to actually get the robot to move in a given direction requires some calculations to be made. The fact that this cannot be implemented without mecanum wheels is also problematic. A major detractor for this design is that roller wheels which are required for this to operate severely limit the robot's traction.

Swerve Drive

Swerve drive robots use wheels that can rotate independently about the vertical axis. The concept is the same as a castor wheel, except that the orientation can be actively adjusted. The angle of each wheel may be controlled individually, in pairs, or all simultaneously. The system requires separate motors for driving the wheels and adjusting the angle of the wheels. Any number of wheels can be used, but four or six are most common.

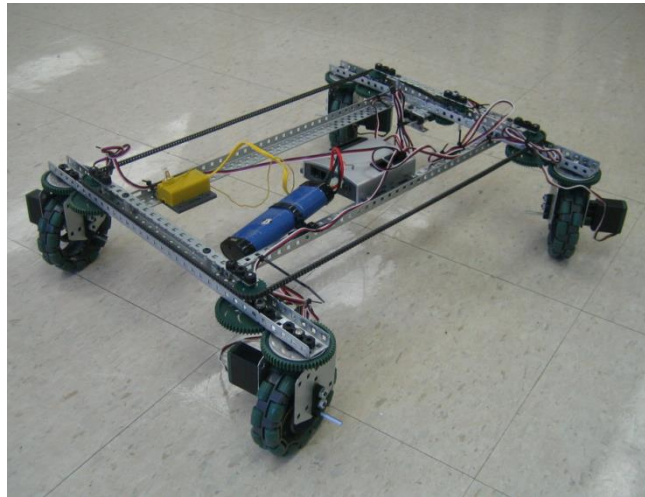


Figure 4: Swerve Drive Frame

Easily controlling a swerve drive system can be complex. Adjusting each wheel separately requires many inputs and is not intuitive. Coordinated motion can be achieved through several configurations. The first involves all wheels pivoting together at the same angle, and allows the robot to move in any direction without changing the orientation of the chassis. Alternately, the front and rear wheels can pivot in opposing directions to allow for small-radius turns. Positioning all wheels perpendicular to the center of the robot allows for zero turn radius. A simpler version involves only rotating the front wheels, like a car. Since the wheels are controlled separately, the functionality of Ackermann steering can be mimicked. Swerve drive systems can also be treated

exactly like tank-drive systems by allowing the wheels to remain parallel to each other and driving one side faster or slower to turn.

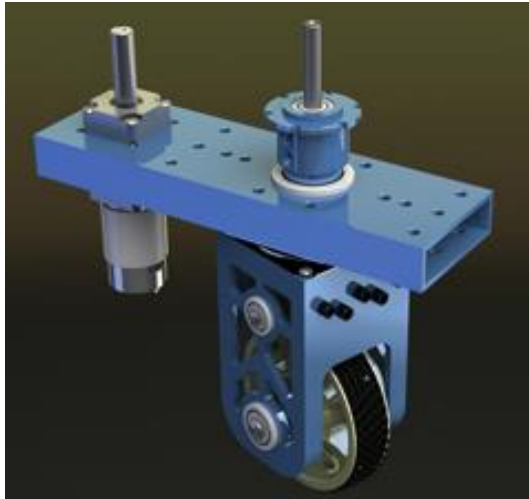


Figure 5: Swerve Drive - Close-up Configuration

Swerve drive systems are favored for their extreme adaptability. Since the wheel positions can be changed in real time, the robot can quickly be optimized for different kinds of performance. The system is generally very maneuverable, and can also achieve high speeds and solid pushing force. However, there is some delay while the wheels are being rotated. The wheel units are relatively tall, which means that the robot will have a high center of gravity and can be unstable. Swerve drive is also mechanically complex, heavy, and requires two motors for each wheel. Controlling these systems also presents a challenge, since so many inputs are required to achieve coordinated motion.

Tank Drive

Tank Drive is a simple system with an independent set of wheels on each side of the robot. This can mean two or more wheels on each side, or an actual tank tread. The left and right wheels are driven separately, so one side can run faster than the other. When both sides are driven forward at the same speed, the robot moves forward. If one side is driven slightly faster than the other, the robot will move along a gradual arc. If one side is completely stopped or driven backwards, the robot can turn in place.

Tank drive is favored because it is extremely simple and inexpensive to build and program. Driving this system is very intuitive, and it can also achieve fairly high speed and good pushing

force. The downside is that this driveline requires the wheels to slip and skid frequently, which drains power and makes it slightly less agile.

Chassis Steering

Traditional Zero-Turn Mowers

Several currently available lawn mowers implement zero-turn systems, allowing them to execute very precise maneuvers. These setups use dual rear transmissions that distribute power to the rear wheels independently, while the front wheels are casters that can rotate freely. Pushing both levers forward causes the mower to move forward, while pulling them back causes it to reverse. Turning is achieved by pushing one lever farther than the other.



Figure 6: Traditional Zero-Turn Lawnmower

The casters used on zero turn mowers can cause issues. When the rear wheels begin a turn, they have to overcome resistance found in the front casters. This can lead to plowing in the front wheels, and when the front casters hold fast, the rear wheels can lose traction. This leads to skidding and slipping. Depending on the make and model, these mowers can also be unstable on slopes greater than 10 to 15 degrees.

Synchro-Steer

Synchro-Steer is a proprietary solution to the caster wheel problem found in zero turn mowers. It still uses dual rear transmissions that distribute power to the rear wheels independently. Instead of two lap bars, these mowers have regular steering wheels. To avoid the issue of the wheels holding fast, the turn is initiated at the front wheels and the speed is controlled at the rear wheels. This is achieved by a pair of linkages between the steering box and

the rear transmissions. Rather than using casters, the front wheels are turned by the steering wheel. When the steering wheel is turned clockwise (for example) the front wheels turn right, and the power to the rear right wheel is decreased. The rear left wheel then pushes the mower through the turn. This allows the mower to make zero radius turns intuitively in any situation.

FIRST Robotics

For Inspiration and Recognition of Science and Technology (FIRST) is an organization founded by Dean Kamen. The organization, which was developed in 1989, is used to promote and encourage students to enter engineering and technology based fields. The robotics side of the organization is an international competition for high school students to compete. For this competition, teams enter a robot which must be able to complete certain tasks for a game which is determined every year. The robots must meet the rules and standards set forth by the FIRST organization.

FIRST Constraints

Our group has decided to use the constraints set by the FIRST Robotics Competition for our robot. Not only will this allow our design to be potentially used by future FIRST robotics teams but it will also determine our constraints instead of arbitrarily coming up with our own. The constraints determined by the FIRST organization cover a vast majority of the robot size and weight specifications. Many of these regulations ensure that the robots entered are safe to handle and fit particular size requirements. The rules described below are in regards to the rules for the 2013 game, Ultimate Ascent.

These rules pertain to the size and weight of the robot. The robot should have a perimeter that does not exceed 112 inches. The robot must also fit inside a 54 inch diameter cylinder. The height shall not exceed 54 inches and the weight should be less than 120 pounds. The weight measurement does not include the battery, cables pertaining to the power system, and the bumpers.

The FIRST constraints will also give us a list of acceptable parts that can be added to the robot such as sensors, motors, and controllers. This list of parts mainly applies to the accepted motors. All electrical components used on the robot must also fit into the rules in regards to wiring and their perspective actions.

Team 190 Survey

Since our group does not have any experience with FIRST or working within the guidelines set forth by FIRST, we decided to go to one of Worcester Polytechnic Institute and Mass Academy's, FRC Team 190's meeting. This allowed us to ask a few questions about robots designed for FIRST Robotics Competitions. The questions dealt purely with the driveline of the robot, which gave us a better idea of how much the driveline should weigh, what is the current preferred driveline, and general performance of other drivelines used.

Past FRC Designs

In FIRST Robotics Competitions, many types of drivelines are used for the various types of challenges that are created. The specific choice of what driveline to use is based on the needs of the game created for that year's competition. Most designs for the drivetrain focus on higher pushing or pulling power as most of the games have some portion where an object must be moved in some way, be it pushing, pulling, carrying, or some other method. The needs for high speeds or maneuverability in the driveline design are also determined based on the goals of the game. Most designs focus on either one of these based on the plan for the robot in the competition. For the most recent 2013 game, teams were challenged with creating a robot which could collect Frisbee discs and shoot them into various elevated goals in order to score points. A secondary objective was to climb a pyramid structure in order to obtain more points by climbing higher up. For example the figure below shows the robot designed by Lynbrook Robotics, "Ultimate Funky Object," for the 2013 competition.



Figure 7: 2013 "Ultimate Funky Object" by Lynbrook Robotics

This drivetrain is a 6-wheel chain drive design which is capable of 15.7 feet per second. The wheels are powered using 4 CIM motors and the gearbox used quickly shifts using servo motors with feedback and synchronization. While this design is capable of high straight line speed and zero-radius turning at a standstill, there are still some drawbacks of this design. At high speed this design does not turn well due to the wheel configuration. It is also incapable of any form translational movement meaning that the most effective way to drive this robot is drive in straight lines, turn at a standstill, and continue on a desired path. For the game this was designed for, this design was effective because it was quickly able to gather disks, move to within range, and rotate the base in order to shoot and score points.

For the 2008 game, one of the challenges was to race around an oval track where completing laps earned teams points. The robot in Figure 8, "Tumbleweed," was designed by Team 148, Robowranglers, with racing the course as its main goal.



Figure 8: Robowranglers 2008 FRC Robot, "Tumbleweed"

This robot implemented a 3-wheel swerve drive to their nonagonal chassis. The wheels are arranged in a triangular pattern. Due to the swerve drive, this robot was capable of very good low speed maneuverability and was capable of translational motion even at higher speeds. The "Tumbleweed" fared well in this game because it was quickly able to maneuver around the oval course due to its high mobility. However, due to the configuration of the wheels, the robot would often tip as it cornered because the one wheel which would end up on the inside of the turn would lose traction and leave the surface slightly. The best way for turning this robot was to have the robot maintain the same direction but rely on translational movement to make the full

turn. While this was effective for the challenge, in many other applications forcing translational movement to turn around corners is sub optimal.

While these are just two examples of different robot designs for FRC, it provides some important information regarding the differences of FIRST drivetrains and the drivetrain we will build. The drivetrains used for different games are efficient because they are used to accomplish certain goals for the challenge provided. However, these drivelines are not optimal as many sacrifices are made due to time constraints and a need for simplicity. Therefore it is important to recognize that while our design will use FRC design constraints, the driveline is not being made for a FIRST competition. Sub-optimal drivelines will do just fine for most FIRST games but that is not the goal of this project.

Design Goals

Primary Goals

The concept of creating an optimal driveline is a very vague one. In order to make this objective achievable, we must set design goals for us to be able to objectively determine that an optimal driveline had been created. For our project, there are two main goals which must be achieved in order to classify our design as optimal. They are stability at high speeds and maneuverability at low speeds. These two goals are still unspecific, so we have generated criteria on which to grade success in these areas.

High-Speed Stability

For high speed stability, we have determined based on research into FIRST robotics competitions that maintaining a speed higher than 10 feet per second can be classified as high speed. With this definition of high speed established, we aimed to create a device which is capable of two main operational goals at high speed. First, our drivetrain and chassis will be able to maintain our definition of high speed around a circular path of a 4 foot lane with a 10 foot radius. This test will prove that our design can maintain a constant turn radius without jerking motions or the need to reposition. The radius of the circle was determined based on the 2008 FRC game "Overdrive" where the robots raced around a track on which the maximum turn radius was 13.5 feet. Secondly, to test other practical high speed maneuvers, we decided to create a slalom course on which to race FIRST robots. We gathered a group of FRC drivers with various degrees of experience and have them drive the course several times, with our design and with a driveline used by WPI and Mass Academy's Team 190 in a previous competition. We hoped that the majority of the selected drivers would finish the course faster with our design than with Team 190's driveline. By succeeding in both these tasks, we could successfully say our driveline achieves high speed stability.

Low-Speed Maneuverability

To establish low speed maneuverability, the driveline must be capable of specific operations at a standstill or very low speeds. First, our driveline will be capable of zero radius turning about a point within the chassis. This will insure that our design has great maneuverability at a standstill. Second, we wanted the driveline to be capable of precise movements at low speeds. This can be accomplished with a design that is capable of translational movement. However, translational movement is not a requirement because with zero radius turning capability and straight line movement, we feel that these precise movements are also feasible. With these objectives achieved, we can assure that our driveline has low speed maneuverability.

General Goals

Finally, there are some general goals we have established based on the FRC constraints and engineering efficiency. We will maximize the tractive forces especially at low speeds and maximize the energy efficiency of the driveline. The most effective way to do this is to make all wheels driven and limit wheel skid. Our design will also comply with all FRC robot design

constraints from the 2013 competition. The target weight of the drivetrain and chassis is 130 lbs., so that our robot is comparable to a 2013 FRC robot with bumpers and battery. We will also aim to make the system as simple as possible. This can be achieved by minimizing the number of motors in the design, limiting the degrees of freedom, and creating an intuitive user interface for driver operation.

By achieving these goals, we can successfully say that we have created an optimal driveline which is proficient in high speed stability and low speed maneuverability. The general goals will also play a major part in the design selection and building process. While some of these general goals are not quantifiable, they will rate highly in importance during the design process.

Primary Goals:

- High Speed (10 feet per second)
 - Maintain 4 foot lane driving a 10 foot radius circle
 - Complete a slalom course faster than traditional FRC190 robot
- Low Speed
 - Capable of zero radius turning

General Goals:

- Maximize traction at low speed operation
- Maximize energy efficiency
- Comply with all 2013 FRC design rules
 - Maximum weight and perimeter of robot
- System will be as simple as possible
 - Minimum number of motors
 - Limited degrees of freedom
 - Intuitive driver operation

Project Design

Design Selection

One of the most important components of the design for our driveline is the configuration of the steering arrangement. It is important to realize that we must be able to obtain the different operational goals from the steering setup as well as maintain a low level of complexity in order to limit the degrees of freedom and make manufacturing simple. Early on in the design process, we felt that the goals of high speed stability and low speed maneuverability could be achieved through a purely mechanical steering system. From our research into the many types of drivelines we came to the conclusion that there were two steering methods which were able to most effectively achieve one of our operational goals but not the other. We found that Ackermann steering systems were the best for high speed stability, as seen by the fact that most motor vehicles have some form of the Ackermann steering principle. However, Ackermann systems were flawed in low speed maneuvers as the turning capability is limited by the geometry. At low speeds we believed swerve drive systems were the best for precise turns, especially zero radius turning. The swerve wheel modules have a full 360° range of motion which allow for very precise movements, but are hindered by the fact that intricate movement capabilities are only possible with sophisticated coding and intuitive remote control. The goal was to find an effective medium between these two in order to achieve the simplicity and robustness of the Ackermann system along with the high mobility of the swerve system. The end result is the design for an “Enhanced Ackermann” system. In Table 1 below we have shown all the different factors that affected which system we felt was the best, with the categories sorted from most to least important.

Table 1: A list of all the different factors that affected our choice of system.

Design Specs	Mike	Steve	William	Kirk	AVG
Must comply with FRC size constraints: 112 in. perimeter, 54 in. side, 84 in. height	5	5	5	5	5
Must be capable of a speed of 10 ft/s	5	5	5	5	5
Must have high speed stability based on our definition	5	5	5	5	5
Must have low speed maneuverability based on our definition	5	5	5	5	5
Should have less than 8 motors	4	5	5	5	4.75
Should have little to no time delay transitioning between high speed and low speed maneuvers	4	5	5	5	4.75
Should maximize programing efficiency	4	5	5	4	4.5
Must have an intuitive user interface	5	4	4	4	4.25
Must weigh less 60 lbs.	4	4	4	4	4
Should maximize use of mechanical control	4	4	4	3	3.75
Must Cost less than \$1600	4	2	4	4	3.5
Should have all wheels driven	2	3	4	3	3
Should have low center of gravity	3	3	3	3	3
Should have no wheel skid	2	3	3	3	2.75

Once we had decided how much to weight each factor we then used them to determine which of the systems we were choosing would be the most ideal. Table 2 below is the result of this, and what determined our final decision. When you look at the table the value immediately associated with each of the design specifications and a particular design is a rating from 1 to 5. The D column on the right is what that design scored for after the weights from Table 1 were applied to its score. Below each of the designs is their total score.

There are also four steering mechanisms on Table 2, "Front Wheel Swerve", "Front Wheel Trapezoidal Steering, Rear Wheel '2-state'", "Front Wheel 'Super' Ackermann via linkage", and "Front Wheel 'Super' Ackermann via gears." The first, "Front Wheel Swerve," is simply a mechanism with two fixed back wheels and two swerve wheels in the front, which electronically replicates our final solution. "Front Wheel Trapezoidal Steering, Rear Wheel '2-state'" is a system where we would have a linkage system in the front, and then allow the back wheels to turn only to a position 90° from the straight position. This would have allowed us to turn about a position in the center of the robot, but with costs

elsewhere. “Front Wheel ‘Super’ Ackermann via linkage” is the design that we eventually decided to go with, and is detailed later in this paper. Finally, “Front Wheel ‘Super’ Ackermann via gears” is our outlined solution, except that rather than a system of linkages we would have tried to use gears directly in contact with the front wheel modules to turn them.

Table 2: This table shows all the factors that affected our choice of driveline system, how we weighted them, and what their total values were. The D values were what the score of each category was after the weighting from the previous table was applied to them.

Design Specs	AVG	Front Wheel Swerve	Front Wheel Trapezoidal Steering, Rear Wheel "2-state"	Front Wheel "Super" Ackerman via linkage	Front Wheel "Super" Ackerman via gears	D1	D2	D3	D4
Must comply with FRC size constraints: 112 in. perimeter, 54 in. side, 84 in. height	5	5	5	5	5	25	25	25	25
Must be capable of a speed of 10 ft/s	5	5	5	5	5	25	25	25	25
Must have high speed stability based on our definition	5	5	5	5	5	25	25	25	25
Must have low speed maneuverability based on our definition	5	5	5	5	5	25	25	25	25
Should have less than 8 motors	4.75	4	3	5	5	19	14.25	23.75	23.75
Should have little to no time delay transitioning between high speed and low speed maneuvers	4.75	4.25	2	4.5	4.5	20.187	9.5	21.375	21.375
Should maximize programing efficiency	4.5	2.666	2.5	4.5	4.5	12	11.25	20.25	20.25

Must have an intuitive user interface	4.25	4.75	1.75	4.5	4.5	20.187	7.4375	19.125	19.125
Must weigh less 60 lbs.	4	5	5	5	5	20	20	20	20
Should maximize use of mechanical control	3.75	1.875	3.5	4.0625	4.375	7.031	13.125	15.234	16.406
Must Cost less than \$1600	3.5	5	5	5	5	17.5	17.5	17.5	17.5
Should have all wheels driven	3	5	5	5	5	15	15	15	15
Should have low center of gravity	3	3.75	4	4	4	11.25	12	12	12
Should have no wheel skid	2.75	5	5	5	5	13.75	13.75	13.75	13.75
TOTAL		255.9	233.8	277.9	279.1				

Mechanical Systems

Steering Assembly

The general idea for an Amplified Ackermann system is to create a standard Ackermann system with a normal range of motion and amplify that range of motion using a chain and sprocket system in order to obtain steer angles which are greater than the steer angles which the normal Ackermann system is capable of. Using a standard swerve wheel module, we have the capability of turning the wheels a full 360° through a purely mechanical setup. By making the driveline front wheel steered, we are able to achieve this very wide range of motion using only a single motor for turning and one motor for each of the driven wheels, 4 in the case of our design. With this configuration, we believe we have an uncomplicated system which maintains the best aspects of swerve and Ackermann steering while being able to accomplish our operational goals.

We chose to use four wheels in the driveline with each individually driven to maximize the traction of our driveline. Another decision was to make the driveline steer using only the front wheels while the back wheels remain stationary. This means that the turning radius will always remain on the line generated by the rear wheels. Through the programming of the controls, this allows us to operate the driveline with only two needed inputs: throttle and steering.

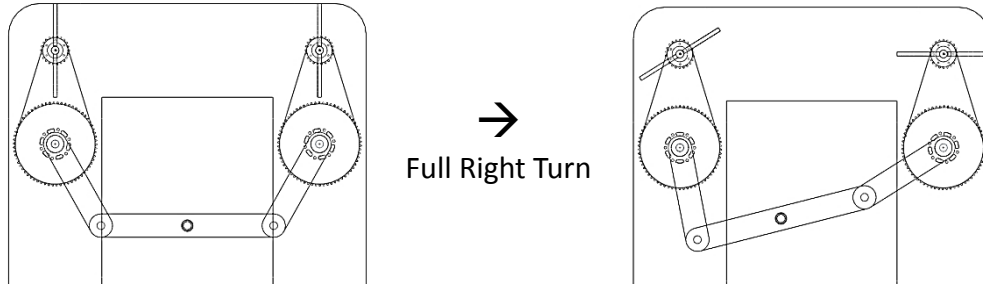


Figure 9: Conceptual amplified Ackermann steering

Figure 9 shows a simplified version of the trapezoidal linkage assembly and chain and sprocket assembly used to attain the Ackermann steering principle. As the linkage is shifted to the left, the large sprockets turn the chains which turn the small sprockets which turn the wheels in order to perform a right turn. To achieve the zero radius turning we have designed the mechanism in order to turn about one back wheel while performing a full left or full right turn. This means that the vehicle must be capable of an inner steer angle of 90° . During a left hand zero radius turn, the driveline will rotate about the back left wheel. Conversely, the vehicle will rotate about the back right wheel during a right hand zero radius turn. This can be seen in the following figures. Wheel velocities must also be individually controlled to remove any skidding which could occur. With each wheel being individually driven, a velocity must be set so that each wheel point maintains the same rotational velocity about the turning center. This algorithm will be explained in more detail in the Motor Control section.

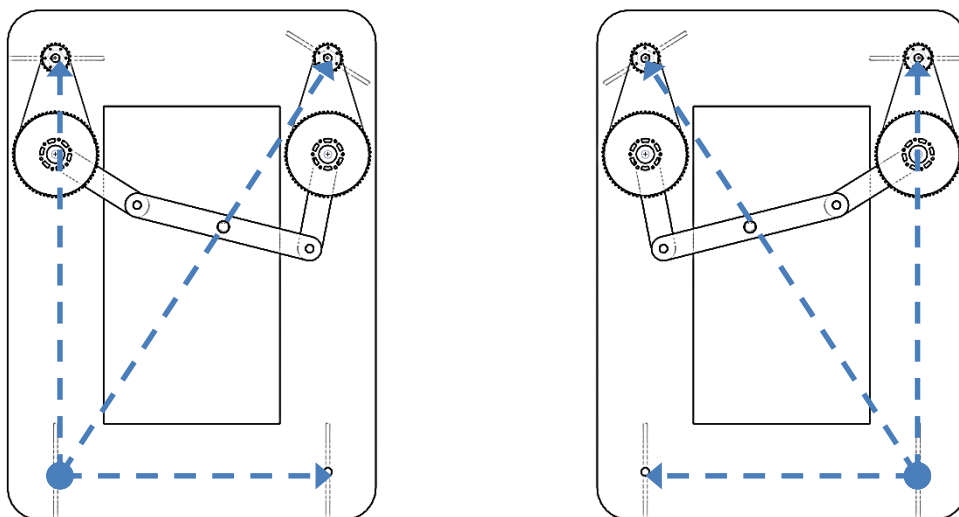


Figure 10: Zero radius turning conditions

This operational decision was made because we feel it allows the driver of the vehicle to easily orientate the driveline purely by seeing the motion of the vehicle. The driver can see if they are turning full left or right based on the wheel about which the driveline is rotating. This also allows the driver to visually see that driveline is moving in forward or reverse configuration even in zero turn radius operation. With this setup, it also means that all wheels will be operating in the same direction at all times except at zero radius where one wheel will be stopped. However, the linkage system can be optimized so that the zero radius turning point is anywhere between the back wheels. This change will also make the steer angle error slightly bigger in the middle ranges.

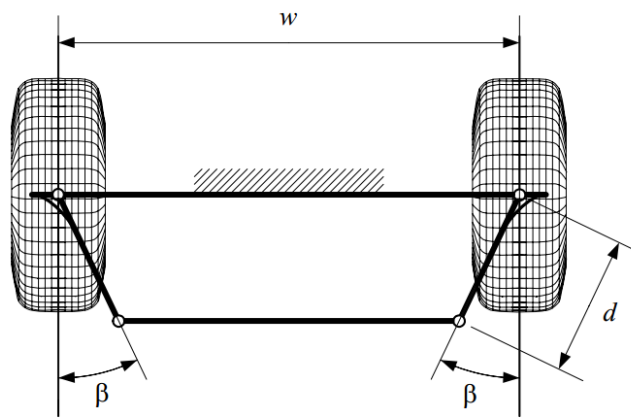


Figure 11: Trapezoidal steering geometry

For this system to work properly, the trapezoidal linkage system, shown in Figure 11, must be optimized for the smaller steer range desired. This linkage system is used to approximate the Ackermann steering condition as a linkage system cannot be designed to create the perfect Ackermann condition. Using the following equations, the outer and inner steer angles can be calculated for the perfect Ackermann condition and the designed linkage system as well as the error between the two:¹

$$\cot(\delta_{A_o}) - \cot(\delta_i) = \frac{w}{l} \quad (1)$$

$$\sin(\beta + \delta_i) + \sin(\beta - \delta_{D_o}) = \frac{w}{d} \pm \sqrt{\left(\frac{w}{d} - 2 \sin \beta\right)^2 - [\cos(\beta - \delta_{D_o}) - \cos(\beta + \delta_i)]^2} \quad (2)$$

$$e = \sqrt{\frac{1}{n} \sum_{i=1}^n (\delta_{D_o} - \delta_{A_o})^2} \quad (3)$$

¹ http://www.idsc.ethz.ch/Courses/vehicle_dynamics_and_design/11_0_0_Steering_Theroy.pdf

Equation 1 presents the condition for the perfect Ackerman system. δ_{Ao} represents the Ackermann outer steer angle while δ_i represents the inner steer angle. The second equation is for the design of the trapezoidal geometry where δ_{Do} is the designed outer steer angle which is generally slightly different than the perfect Ackermann condition. β is the angle at which the linkage bars connect to the tie rod as shown in Figure 11. For both equations, the outer steer angle is calculated over a range of inner steer angles. For n values of δ_i we can then find the error for a specific β in the trapezoidal geometry. For all equations, w , l , and d represent the wheel track, wheelbase, and linkage length respectively.

For our specific design, we must keep in mind that the steering angles are being amplified by the chain system. We have designed the system with a gear ratio of 3:1 using VEXpro #25 sprockets of 66 teeth and 22 teeth. With this ratio we must then design the trapezoidal geometry to be effective for an inner steer angle up to 30° , a third of the amplified 90° steer angle. For the calculations we have also chosen the following values for the design: $w = 17$ in, $l = 26$ in, and $d = 6$ in. There are many different ways the β value can be optimized and one would be to choose a value which would result in the lowest error. However, because we want to be sure we have the zero turn radius established about the back wheel, we calculate β from Equation 2 assuming $\delta_{Do} = \delta_{Ao}$ when the inner steer angle is 30° . This way we can assure that the linkage system is perfect at 3 conditions: straight, full left, and full right. We find that $\beta = 29.246^\circ$ and calculate the tie rod length to be 11.137 in. With this β value established we can then calculate the error for the amplified system from the equations. Figure 12 shows a graph which compares the amplified system we have created to the perfect Ackermann condition over the same range of inner steer angles. It must also be noted that all steer angles must be multiplied by 3 due to the amplification process.

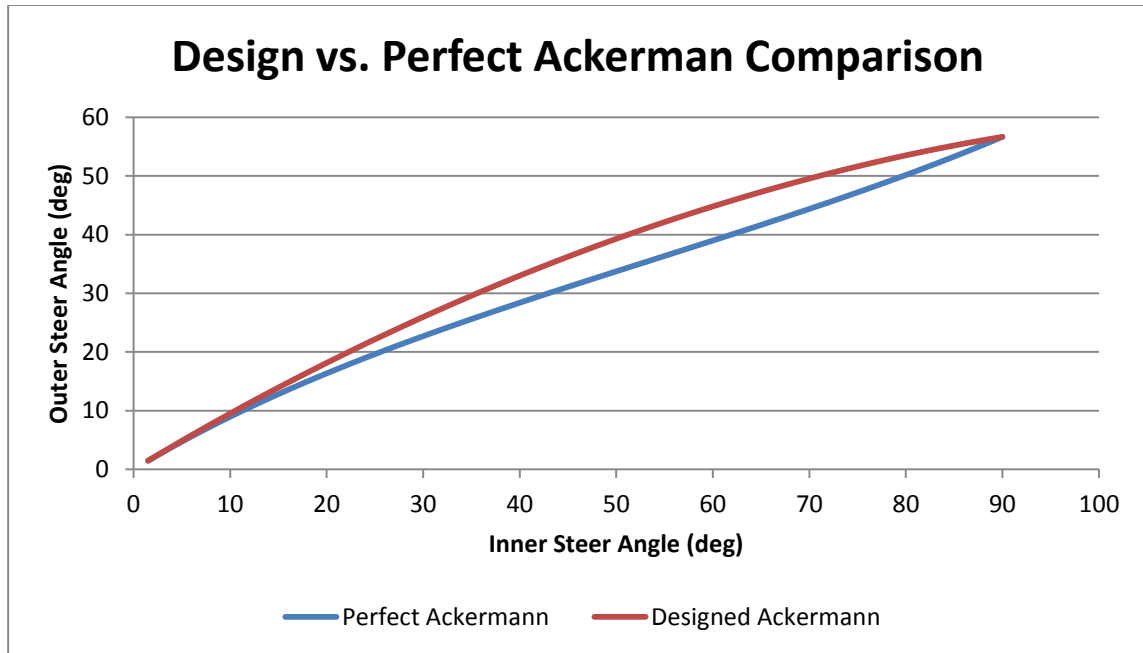


Figure 12: Designed versus perfect Ackermann plot

From the chart, we can see that designed steering system (red) has outer steer angles slightly higher than the perfect Ackermann condition (blue). However, at both extremes the amplified system becomes equal to the perfect case. The root-mean-square error turns out to be 3.9° while the maximum error is 5.82° . We feel that this error is tolerable as it will have an almost negligible effect on the performance of the driveline.

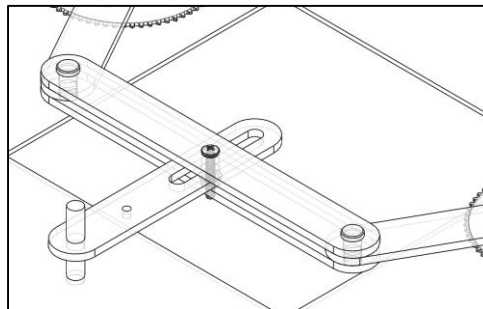


Figure 13: Conceptual steering arm design

In order to properly steer the driveline, we must implement a way to actuate the linkage. To do this, we chose to use a steering arm connected to the center link of the trapezoidal linkage which can rotate the linkage in either direction, shown in Figure 13. The arm is connected to the center link using a pin-in-slot joint because the rotation of the center link using one point of contact does not have a constant radius. Two center link parts must be created so that the pins which connect the tie rods to the

center link and the pin for the pin-in-slot joint can be supported in double shear and allow for even distribution of forces. Due to the nature of the geometry, the force needed to actuate the linkage is not linear and a much higher force is needed to rotate the arm at the limits of the steering range. Therefore, a high-torque motor is needed to control the steering arm and this will be explained in greater detail in the Motor Selection section.

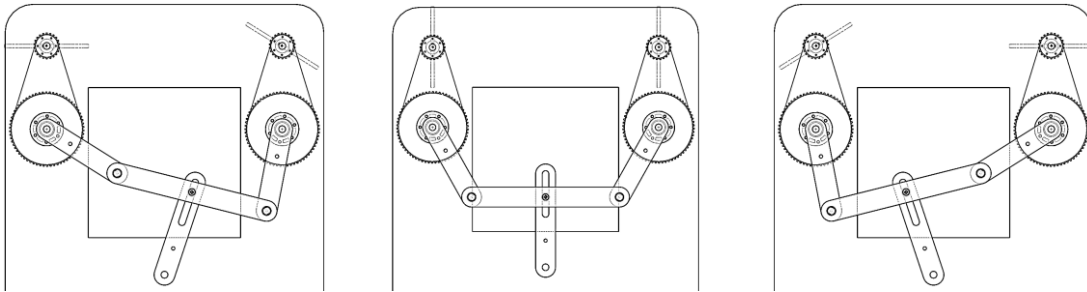


Figure 14: Steering arm range of motion

The linkage system, the 3:1 ratio chain and sprocket system, and the steering arm make up the steering assembly which will allow our driveline to be capable of the desired high and low speed performance.

We determined the coefficient of friction and the weight requirement for our robot, by assuming worst case scenarios. For rubber on carpet we were able to determine that this coefficient would be .65 and we assumed 120lbs of force would be applied directly to each wheel, so that our requirement would be a worst case scenario. We then converted the force to Newtons and multiplied the friction force of .65 which allows us to find the minimum wheel shaft torque needed by assuming the wheels are one inch thick. The minimum torque requirement, neglecting friction in the linkage system, is 4.4 Nm. With the 3:1 amplification ratio we can then find the required torque for the linkage shaft. Assuming that the steering arm maintains a 90 degree angle to the center link, we can then find necessary force applied and resultant torque of the steering arm shaft. For good performance, we decided that the linkage system would need to cover the full range of steer angles in one second. To do this, the shaft's rotational speed would need to be 7.5 RPM. With the rotational speed and shaft torque known, we can find the power needed over the range of steer angles. Figure 15 shows this relationship over the steer angle range of the linkage system where a negative angle indicates an outer steer angle and a positive indicates an inner steer angle. From this we determined that the maximum power needed would be 16.92 W. These calculations can be seen in the Appendix.

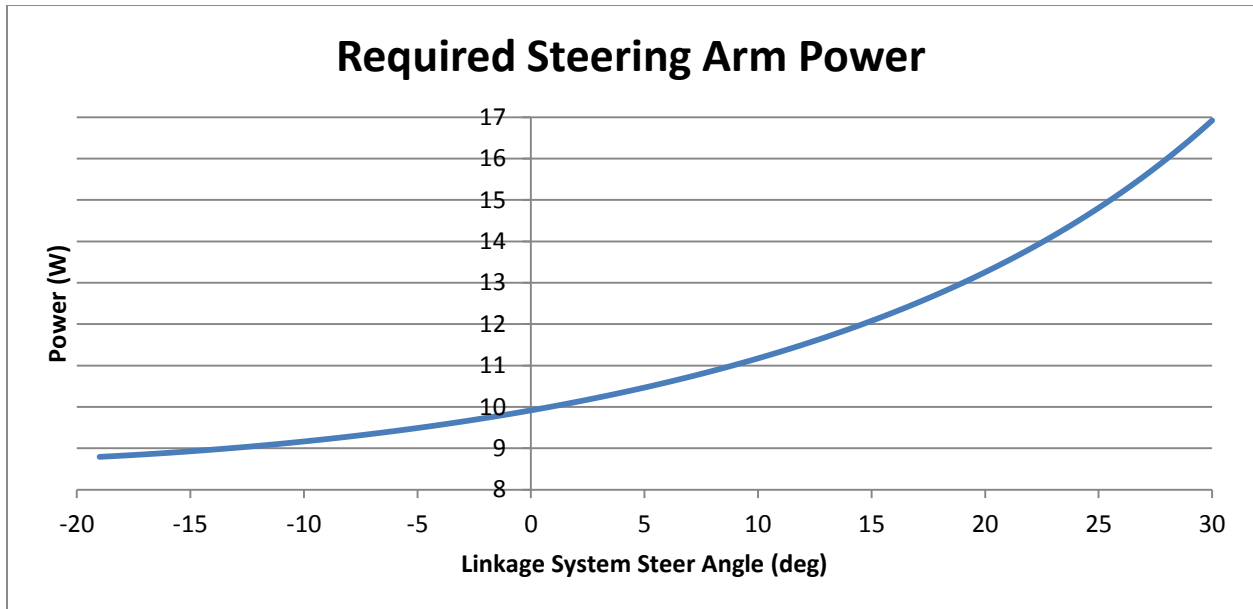


Figure 15: Required steering arm power

Wheel Modules

Requirements

The functional requirements for the wheel module are as follows:

- Back wheels must be fixed, but should use the same basic structure as the front for simplicity
- Front wheels must have a turning range of up to 180 degrees
 - This motion must be controllable via a horizontal chain or belt in order to be compatible with our steering mechanism design.
- Each module must have a CIM motor
- The module must include a gear reduction to achieve our goal of 10 ft/sec
- Must use 6" wheels
- All four wheel modules must support the weight of the robot
- Wheel modules must be solidly mounted to the chassis in such a way that they can have some sideways force applied to them without breaking

Front Wheel Module Design Process

Initially, we considered several approaches to the wheel module. We made rough sketches of a few designs, including different layouts of the gears and CIM motors. Our initial concern was fitting all the components into the module so that the whole thing was as compact as possible.

We decided early on that we wanted to mount the CIM motor inside the module itself rather than deal with the more complex system of transferring the power down from somewhere in the

chassis. This decision avoids a significant amount of gearing, and simplifies the design. Treating the wheel module as a standalone unit (with CIM included), we also needed a way to rotate it via a chain from the steering mechanism. We decided that the best way to do this was to attach a sprocket horizontally at the top of the module. The module would then be mounted to the chassis above that sprocket, using bearings and some sort of vertical shaft.

The next step was to design a gearbox capable of producing the required RPM at the wheel. Since the maximum power of a CIM is delivered when the motor runs at 50% of its free-running speed, we did our calculations based on the motor speed of 2650 RPM. We geared this down so that with 6" wheels (which have a circumference of 18.85") the robot would run at 10ft/s. It is important to note that the robot may be capable of going faster than this, but the maximum power will be delivered at a velocity of 10ft/s. As discussed in the Motor Selection section, we determined that the gear ratio should be 6.95:1. Using this desired gear ratio, we began looking for gears that would achieve this in a two-stage reduction. Initially, we wanted to use one spur gear stage and one chain and sprocket stage. However, we learned that this would require the final small sprocket to have 9 teeth, which is too few. So we decided to go with a three stage reduction of spur gears instead. After discovering that the spur gears we wanted were very expensive, we began to look into off-the-shelf wheel module kits that included gears.

This research opened up new options for the wheel module design. We had already settled on several specifications, and we were able to find wheel module kits that closely resembled what we were planning to build ourselves. The most intriguing was the AndyMark Wild Swerve Module. This module incorporated our ideas about mounting the CIM in the module, using a three stage spur gear reduction, and attaching a sprocket to the top for steering. It used the same 6" wheel and CIM motor combination that we wanted, and had several options for gear ratios. The closest was 6.94:1, which is very close to our desired ratio of 6.95:1. The data that AndyMark provided also confirmed that the speed of the modules with this ratio is 10ft/s at 50% motor speed. This module also introduced us to the idea of having a bottom circular plate held in place by a ring of pads, to support the wheel module from the bottom as well.



Figure 16: AndyMark Wild Swerve Drive Module

Even though our intention was never to use a swerve drive system, the swerve module is actually compatible with our ideas as well. The key feature of swerve drive is the ability to rotate the entire wheel module via a sprocket at the top. While we were not planning to rotate each wheel independently or link them together the way swerve systems sometimes do, we could still use the sprocket to connect the swerve module to our own modified Ackermann steering mechanism.

Since the cost of the AndyMark module was comparable to what we would have spent building our own, we decided to use these instead to save time. We began by downloading the CAD model from AndyMark and disassembling it to gain an understanding of how it worked. We looked into making our own parts to mimic this design, but ultimately decided that we could not build it for significantly cheaper than the off-the-shelf version.

Our focus then shifted to modifying the Wild Swerve module to suite our needs. We had already begun to design a chassis with two horizontal plates that could easily be mounted to the top and bottom support plates of the Wild Swerve module. Aside from mounting the module to the chassis, the other concern was integrating the module into our steering mechanism design. We had already decided that we needed a 3:1 reduction from the Ackermann system to the wheel module. The Wild Swerve module comes with a 36 tooth sprocket for steering. This would have required us to use a 108 tooth sprocket at the other end. Since this was not feasible, we concluded that we would have to replace the module's sprocket with a smaller one.

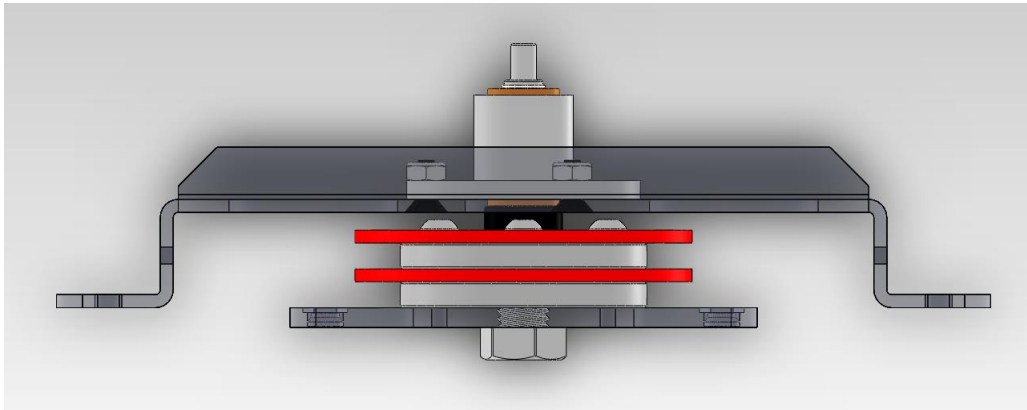


Figure 17: Original bracket assembly

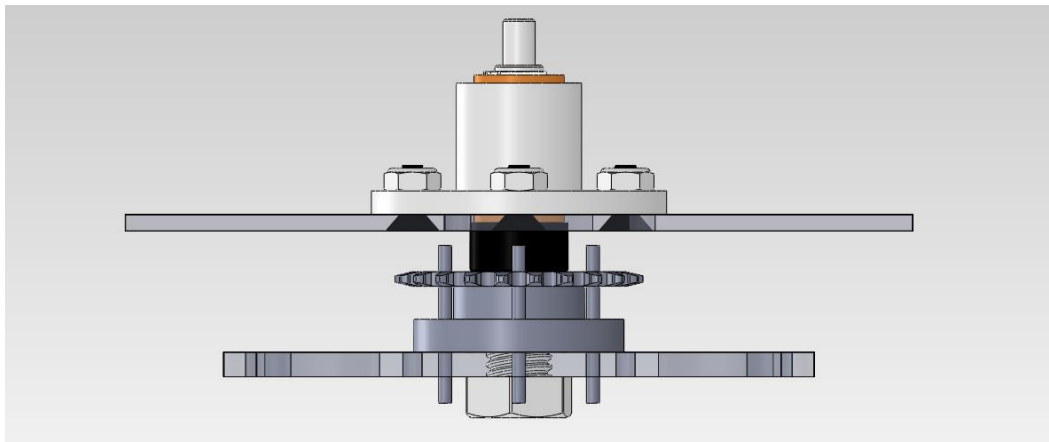


Figure 18: Modified bracket assembly

Our plan up until then had been to use a 14 tooth sprocket on the module. However, because of the way the sprocket had to be mounted to the swerve module, we realized that a 14 tooth would be too small; it needed room for a ring of holes to be drilled through the sprocket to mount it to the module effectively. So we settled on a 22 tooth sprocket on the module and a 66 tooth sprocket at the other end of our steering mechanism.

We then set about designing new parts to mount our sprocket to the Wild Swerve module. We found a solution that involved modifying a few of the parts included in the kit, and machining a new spacer. The final design had the same overall size and clearance of the off-the-shelf module, the same general method for mounting the sprocket, but with a 22 tooth sprocket instead of a 36 tooth sprocket. All other aspects of the Wild Swerve module were compatible with our chassis design.

Rear Wheel Module Design Process

For the rear wheels, which do not rotate, we decided to use a partial version of the Wild Swerve modules. The top assembly that allows the module to rotate could be completely left out, and the top of the gearbox could be directly attached to the frame. On the bottom however, the wheel modules consist of a round plate that rotates within a hole in a larger square plate. In order to make the rear modules more rigid, and not allow them to rotate at all, we needed to replace the bottom plates with a single solid square plate that directly attaches to the bottom of the gearbox. Figure 19 shows the part of the kit that we were able to use for the rear wheels. All other parts needed to be redesigned and manufactured to mount the module to our frame.

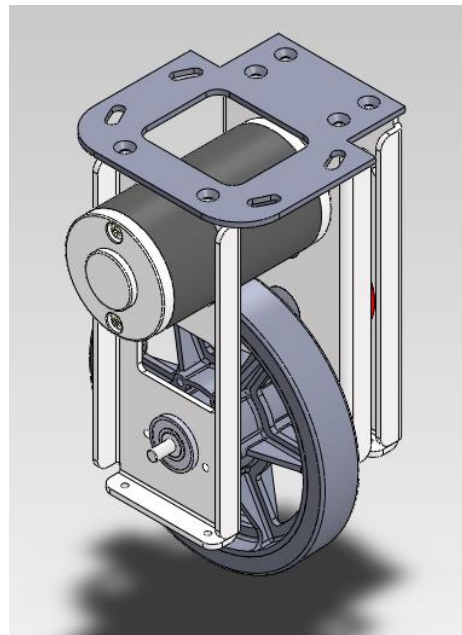


Figure 19: Partial kit for rear wheels

We made a CAD model of such a plate by copying the hole pattern in the circular plate that came with the kit and putting the same holes in a plate with dimensions that matched the outer square plate. This way, we could attach the plate to the partial kit shown above so that it could be mounted directly to the frame at the back of the chassis.

Final Design

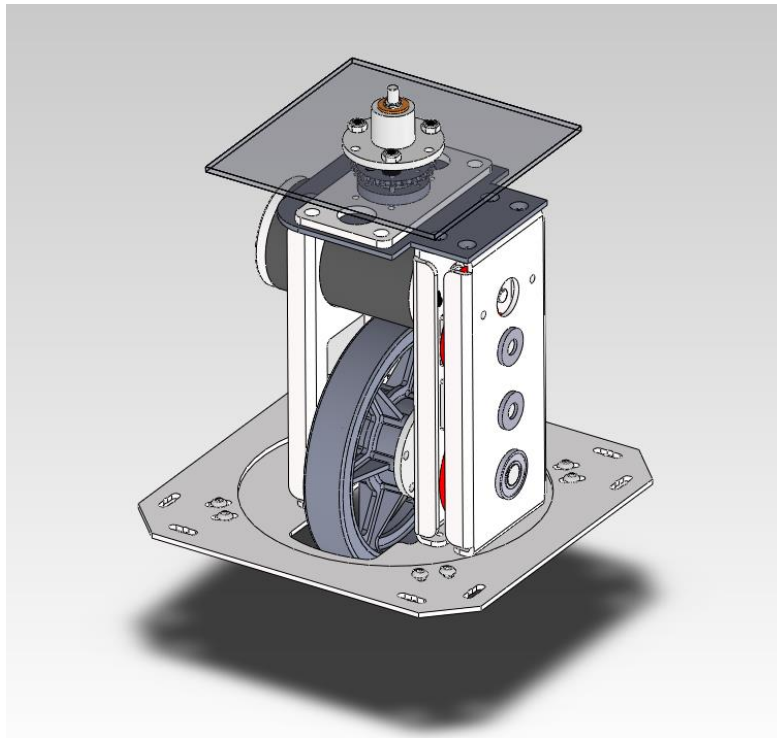


Figure 20: Final modified Wild Swerve module for front wheels

The design for the front wheel modules is an AndyMark Wild Swerve Module with a 6.94:1 ratio, with a few modifications. First, the kit does not include a motor, wheel, or wheel hub. We used a CIM FR801-001 motor, a 6" 2008 FIRST wheel, and a matching 375 Hex Hub. We also needed to buy a new 22 tooth sprocket and drill new screw holes in it. The modified components and the final assembly, are shown below. This assembly was then added to the Wild Swerve module in place of the intended one.

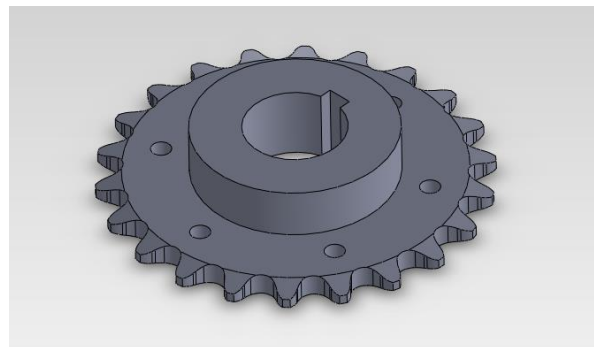


Figure 21: New 22 tooth sprocket with holes drilled

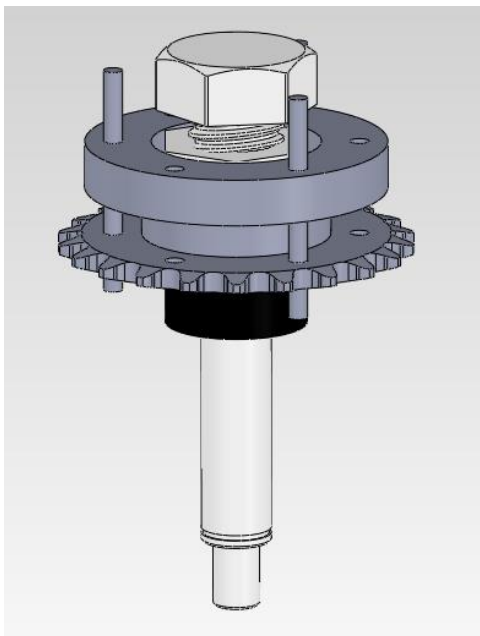


Figure 22: Modified sprocket assembly

For the rear wheels, we designed a different bottom plate to replace the two rotating plates in the kit. This eliminates the ability of the module to rotate. A drawing of the new part is shown below.

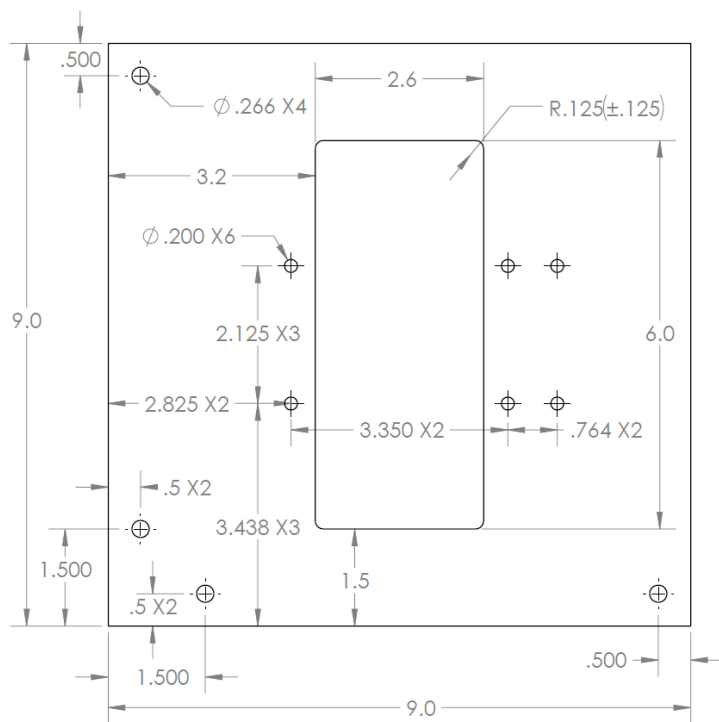


Figure 23: Part drawing for rear wheel module plate

Chassis

Our preliminary plan for the chassis was to simply use two solid aluminum plates. One was supposed to connect to the bottom plates of the wheel modules, and the other would connect to the top wheel module brackets and also provide space to mount the steering assembly. Due to the weight and expense of using this design, we decided to explore other options.

Since we had some success finding off-the-shelf wheel modules, we also researched kits for robot chassis. Because the focus of our project was on creating an innovative driveline, we did not consider the chassis to be a critical part of the design as long as it was compatible with our other subsystems. One promising option we found was the VEX chassis kits, as shown in Figure 24: Off-the-shelf VEX chassis.



Figure 24: Off-the-shelf VEX chassis

Unfortunately, these kits do not come in large enough sizes to support the total size of our robot. We also considered buying two of the kits and combining them, but ultimately decided that this would defeat the purpose of the purchasing a kit to save time.

We designed a basic structure for the frame using VEX parts, because we intended to later find materials with similar dimensions. The frame consisted of a top layer and a bottom layer, with vertical pieces connecting them. Because the tops of the wheel modules would have chain extending backwards, we needed to leave space there. Instead of having a solid bar reach across the entire width of the robot behind the front wheels, we designed a structure to go between the two wheel modules. This provides rigidity to the front section of the chassis and adequately supports the wheel modules.

In addition to the metal frame, we also still needed some sort of platform to mount the steering assembly and other components. For simplicity and adaptability, we decided to use a sheet of high-grade plywood mounted directly to the top layer of the frame. This would allow us to easily drill extra holes later in the build process. There is also a second plywood platform that runs along the length of the bottom layer for mounting the battery and additional weights for ballast. The finished chassis design is shown below.

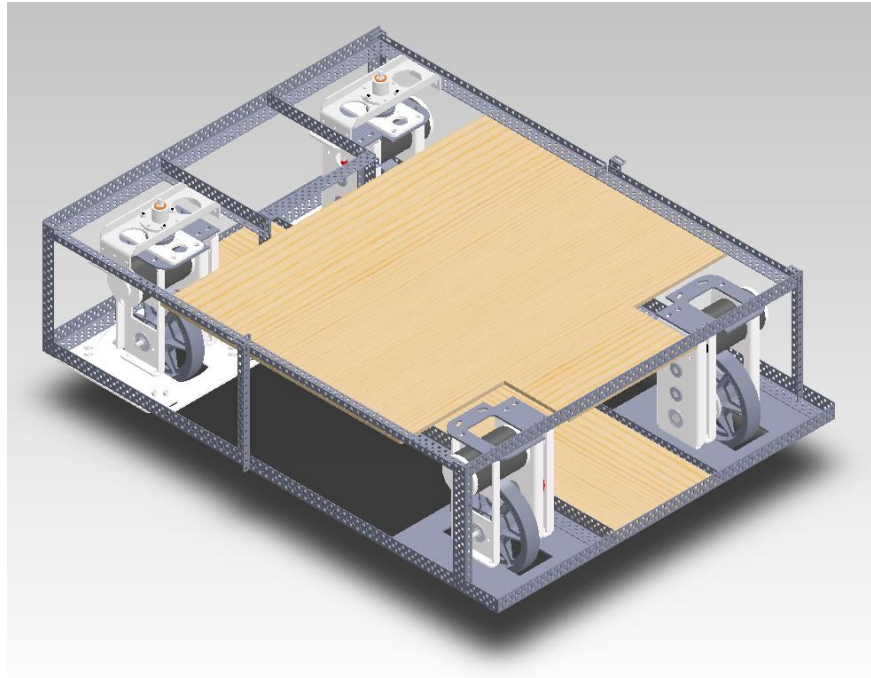


Figure 25: Chassis design with VEX angle bars

After combining the other mechanical subsystems discussed above, we generated a CAD model of our plan for the whole robot. It includes the actual material we used for the frame, the final versions of the wheel modules, the steering linkage, and the top polycarbonate sheet.

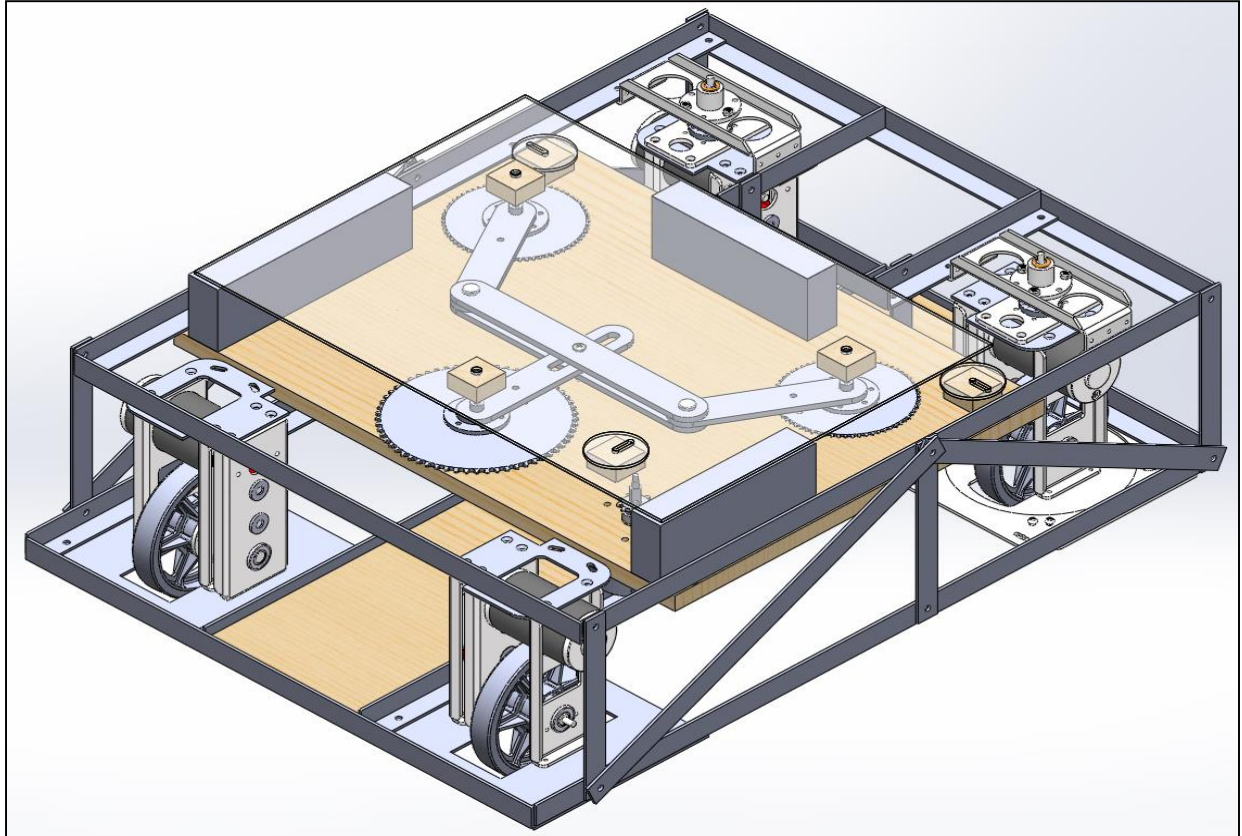


Figure 26: Final CAD model

Electrical Systems

Motor Selections

Motor Controllers

Before we can get into the actual motors we needed to decide on a controller that can handle all of the motors offered by the First Robotics Competition (FRC) and still offer the best bang for the buck. The Talon and the Victor motor controllers are relatively inexpensive but are also very simple in design. The Jaguar motor controller is slightly more expensive than the other two motor controllers and offers more features. These added features would be beneficial for our project but based on reviews and other research that we did, have been proven to be unreliable. Due to this research, we decided to go with the Victor 888 motor controllers from VEX Robotics. The Victors are very reliable and robust which is exactly what we need for our robot.

Driving Motors

The first motor we looked at to drive our chassis was the CIM FR801-001 motor, since it was readily available to us and the robot we would eventually test against would be powered by them as well. For the high speed stability portion of our project, our robot needs to be able to go at least 10ft/s. This motor coupled with the “Wild Swerve” wheel module from AndyMark with the Gear Ratio of 6.94:1 allows the us to produce a speed of 10.4 ft/s which is above the desired of 10 ft/s. The maximum power will be delivered at a velocity of 10ft/s when the motor is running at 50% of its free spin speed.

Turning Motor

Based on our previous calculations of the power required of the turning motor, we knew that we would need at least 16.92W. There were two options that were readily available to us: the Bosch Van Door motor with 53W and the Snow blower from AndyMark with 30W. With the correct gearing, either of these were a viable option. We chose to investigate the Van Door motor first because of its higher power.

We were able to confirm that this motor would perform well by working backwards through the same process that we used to determine the power requirements. We had also already determined that we would have to use a gear ration of 6:1 in order to achieve a speed of 7.5RPM at the base of the steering arm. This is fast enough to drive our linkage rom full left to full right in 1 second. Based on this gear ratio, we found the torque applied to the steering arm. By dividing by the lever arm, we calculated the force applied to our trapezoidal linkage. This can then be used to find the torque applied to the sprockets on the wheel modules with the assumption that the steering arm remains perpendicular to the center link. The minimum torque generated in the wheel module shaft becomes 12.95 Nm which is greater than necessary 4.4 Nm. However, these calculations ignore any friction in our linkage. The plot below shows the torque in both the linkage shafts and the wheel module shafts over the entire steer angle range of the linkage system. These calculations can be seen in the Appendix.

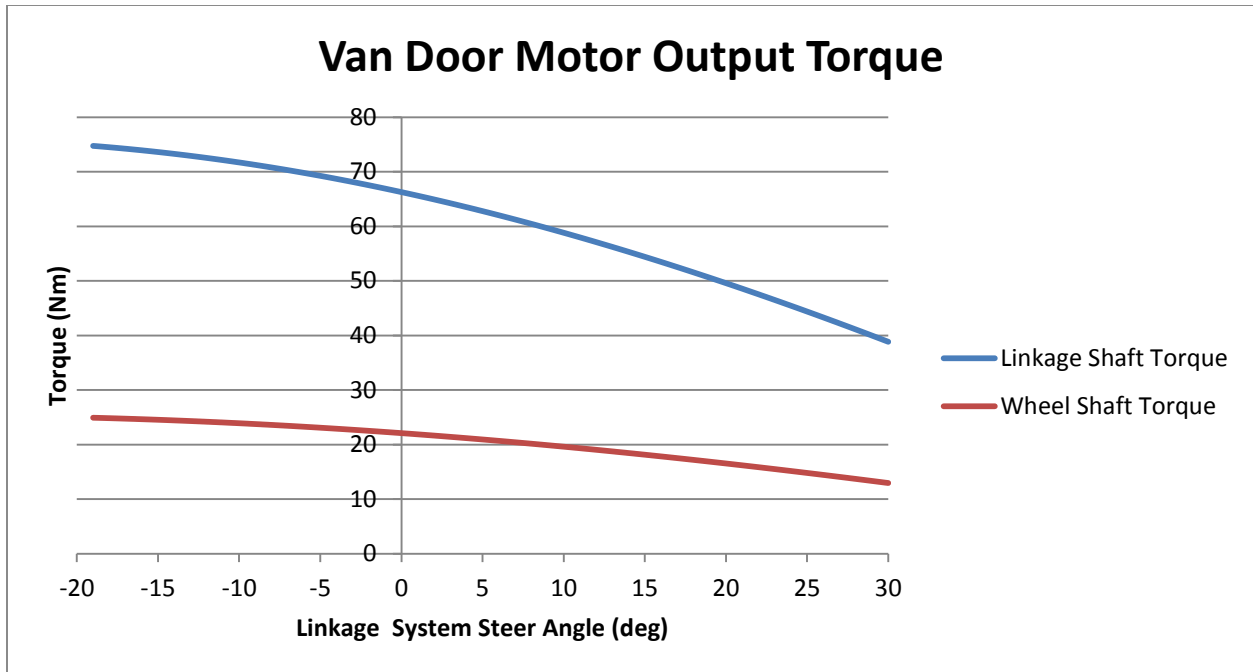


Figure 27: Van door motor output torque

Microcontroller

The Arduino Mega 2560 is the microcontroller that we have chosen for our design. We initially started looking into Arduino microcontrollers as an alternative to the FIRST Robotics cRIO because of the costs; there is approximately a \$700 difference between the Arduino products and cRIO. Once we started looking at the different Arduinos that were available to us we came to the conclusion that the standard board, with only one set of transmit/receive pins and not very many digital ports could prove to be a problem. For this reason we switched to the Arduino Mega 2560 which has multiple transmit and receive ports as well as digital and analog ports. The extensive amount of ports will assist us in having plenty of options and alternatives to choose from. Another major point is that Arduinos have extensive open source libraries that we can take advantage of. This includes some tutorials on how to set them up to run Victors, which will be extremely helpful when we begin the process of wiring and programming our system.

Sensors

We are using several sensors in our design to ensure that we are able to properly control and monitor the various systems, in order to meet the performance criteria we have laid out. For example, it is critically important that we can tell how far our steering motor has turned our wheels to ensure it does not lock up. In order to prevent this we have a potentiometer to measure how far from straight ahead it has turned, with limit switches as a failsafe mounted to the chassis. The potentiometer will also

be able to tell us what degree of turn we are currently making which we can use in our wheel speed algorithm.

The potentiometer we plan to use has a 300 degree range of accurate readings. This will be mounted so that it is turned by our steering motor, and therefore will allow us to keep track of where it is relative to our center, or straight, position. The turning motor we have determined will have to move no more than 270 degrees, and as such the 300 we're able to use with this sensor is more than enough. This potentiometer in particular was chosen for its low price and the ease of acquisition.

Next is a VEX brand limit switch, this will be mounted on our chassis so that our steering mechanism will hit it before it gets so far that it locks up. We will program the switch to prevent the motor from turning any more in the direction that would cause lock up. The motor is allowed to turn away from this point but no further in the limit switches direction if the switch has been activated. We have selected this particular limit switch because of its low cost and ease of use.

Teleoperation

The controller that we have selected to use with our system is a Turnigy 9X 2.4Ghz 9 channel transmitter and receiver with dual joysticks on each side. We will program a setting where the left hand joystick, will control the throttle of the wheels and the right stick will be used for turning. Another nice feature of this controller is that the sticks are self-centering, so we don't have to worry about the driver needing to center the steering and throttle manually. The biggest reason for choosing this controller was because of how common these types of controllers are. This should make it easier for other people to learn very quickly how the robot operates.

Schematic

Below is a basic diagram of the electrical schematic that was used to wire together all of our components.

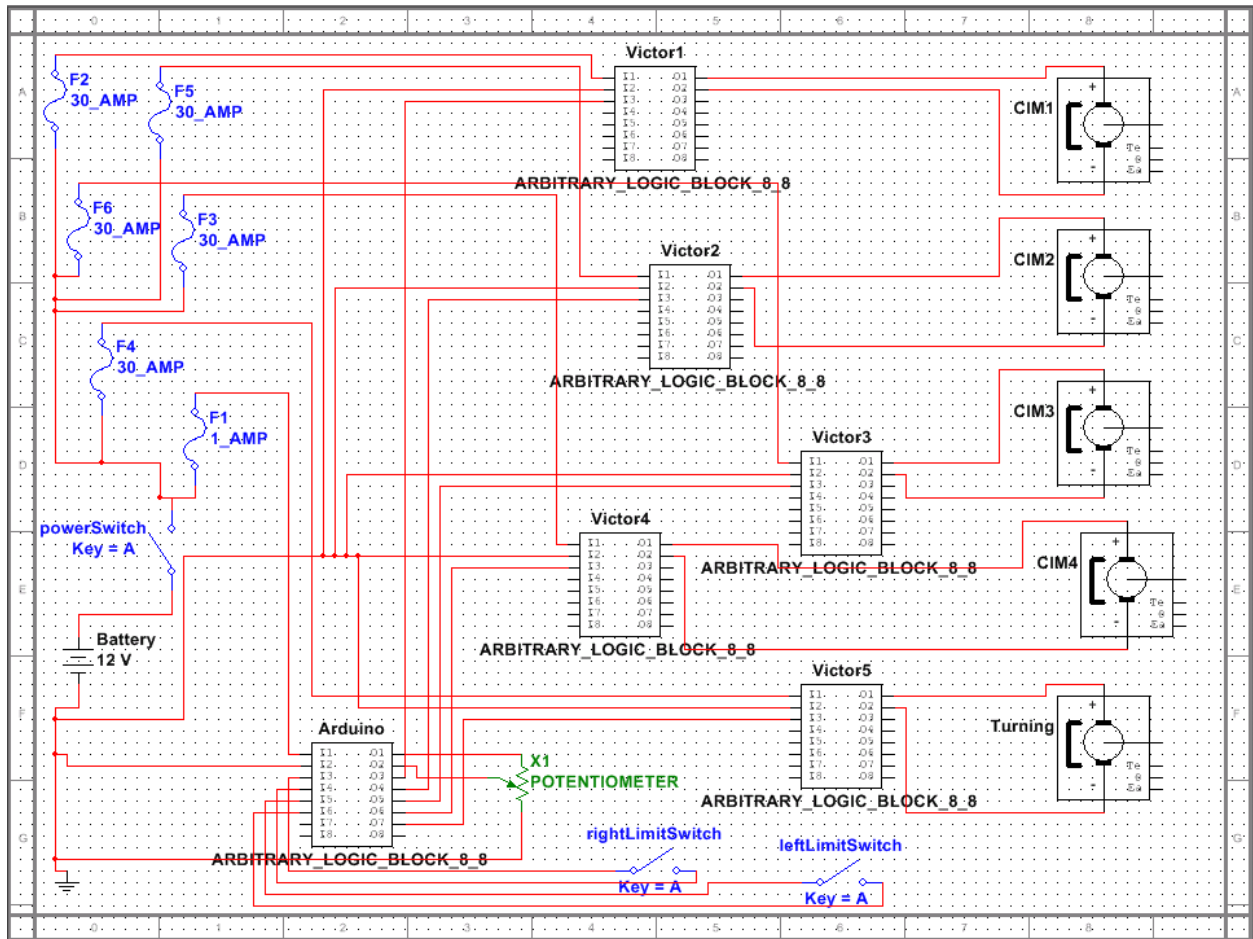


Figure 28: Electrical schematic

Programming

Motor Control

As mentioned earlier, we decided to go with Victor 888 motor controllers. The motor controllers will be wired to the Arduino via 3 wires. These wires will be carrying signal, 5 Volts, and ground. The Arduino will send the Victors signals based on the sensors = A and wheel speed algorithms. These signals will be in the form of Servo values which the Victor will convert to Pulse Width Modulation (PWM) signals.

The four CIM motors that will be used for the wheel modules will receive a signal from their respective Victors based on the wheel speed algorithm. The algorithm will take in the throttle value

from the controller and also the potentiometer value. From these values, the algorithm can then determine which wheel should be spinning at what speed.

The turning motor will operate via Proportional-Integral-Derivative (PID) control. The function in charge of sending the signal to the turning motor takes in the potentiometer value and turn value being sent from the controller. This function then sends the turning motor a signal based on which point on the potentiometer it needs to reach.

Pseudo code

We have outlined below relative functions we will be using with our Arduino Mega 2560 in order for our robot to perform as desired. These functions are setMotorSpeed, getPot, getController and setTurnSpeed. Each of these functions has a particular use that will be combined in order to properly control the various systems we have designed and built into our driveline. Listed below is each of the respective functions in pseudo code as well as a description of how it is intended to work.

The setMotorSpeed function takes in the name of the motor you are adjusting, throttle value from the controller, and the potentiometer value to determine degree of turn. It will be used to tell the microcontroller precisely what speed to send to which controller. Using our wheel speed algorithm, would allow us to create what is essentially an electronically controlled differential.

```
setMotorSpeed (Motor motorNum, int potNum, int throttle) {  
    Set speed based on inputs  
}
```

The getController function is what is used to store the data being received from the controller so that it can then be used by other functions such as the setMotorSpeed function.

```
getController () {  
    Poll controller data. This will listen for commands based on the controller joy sticks  
    and then transfer those into new values for both the steering motor and the drive motors.  
    int left/right;  
    int throttle;  
    throttle = stop;  
    left/right = center;  
}
```

This function, getPotValue, is used to store the current reading of the potentiometer into a variable so that it can be used by other functions.

```
getPotValue () {
```

Poll pot data to be used to determine the location of the steering motor. Will store this in a global variable.

```
int potPosition = potNum;  
}
```

The setTurnSpeed function will set the turning motor to a particular value based on the input from the controller and potentiometer.

```
setTurnSpeed (int potNum, int left/right) {  
    Turns linkage to desired location based on current value and joystick input.  
}
```

Budget

Below is our budget for this project. The Arduino Mega 2560 and Turnigy 9x have costs of \$0 because they were previously acquired by one of the group members. Everything else that has \$0 was loaned to our group from the FRC 190 team or Robotics Engineering Department.

Item	Cost per Item	Number	Total Cost
Victor motor controller	\$65.00	5	\$325.00
MK ES17-12 Battery	\$0.00	1	\$0.00
Arduino	\$0.00	1	\$0.00
CIM FR801-001	\$0.00	4	\$0.00
#25 Chain 10 Feet	\$9.99	1	\$9.99
6 inch Wheels	\$0.00	4	\$0.00
300 degree/one turn pot	\$0.00	1	\$0.00
Bosch Van Door	\$0.00	1	\$0.00
Cotter Pins	\$4.14	1	\$4.14
Clevis Pin	\$8.58	1	\$8.58
Sleeve Bearings	\$0.57	4	\$2.28
Partial Wild Swerve Modules	\$175.25	2	\$350.50
Fuse Block	\$10.61	1	\$10.61
Assorted Fuses	\$21.47	1	\$21.47
Power Switch	\$30.00	1	\$30.00
Aluminum for Machining	\$66.23	1	\$66.23
Full Wild Swerve Modules	\$209.00	2	\$418.00
375 Hex Hub (am-2231)	\$10.00	4	\$40.00
500 Key Hub (am-0077a)	\$10.00	3	\$30.00
#25 Sprocket w/ hub - 22t	\$6.99	2	\$13.98
Vex Limit Switch (2 pack)	\$0.00	1	\$0.00
Turnigy 9x 2.4 GHz Tx & Rx	\$0.00	1	\$0.00
Plywood 4'x8' 5 ply	\$53.09	1	\$53.09
Assorted Fasteners	\$85.40	1	\$85.40
Angled Steel 1/8"x1"	\$87.76	1	\$87.76
Flat Steel 1/8"x1"	\$12.05	1	\$12.05
Flat Steel 1/8"x2"	\$18.00	1	\$18.00
Polycarbonate 24"x24"	\$36.15	1	\$36.15
#35 Sprocket 60t	\$29.21	1	\$29.21
#35 Sprocket 10t	\$10.25	1	\$10.25
Assorted Nylon Spacers	\$6.15	1	\$6.15
#35 Chain 5 feet	\$0.00	1	\$0.00
		Total	\$1,668.84

Figure 29: List of expenses

Manufacturing and Assembly

Mechanical Systems

Chassis

In order to build the frame that we designed previously, we first had to find a material that could fill the role of the VEX bars in our CAD model. We ultimately used steel right angle bars that were 1"x1", and 1/8" thick. While these were significantly stronger and heavier than necessary, we selected them because we were already planning to artificially add weight to make our robot comparable to typical FRC robots that had other equipment besides the driveline. A good way to distribute this extra required weight while also making the robot base stronger was to use an excessively substantial frame material.

We then cut the frame pieces to the required lengths and drilled 1/4" holes in the specified locations, according to the CAD design when it had VEX parts. The frame components were connected at the joints using 1/4-20 bolts and Nyloc nuts. There were slight alignment issues with some of the holes, which we fixed by widening the holes slightly with a Dremel tool. This was most prevalent where the bottom plates of the front wheel modules connected to the frame. Initially, the plates were slightly out of alignment with where the tops of the wheel modules were attached. This resulted in the wheel modules being at a slight angle, which caused a great deal of friction where the round plate of the wheel module came in contact with the sliders on the outer square plate. By making small adjustments to the holes, we were able to perfectly align the wheel modules so that they rotated smoothly.

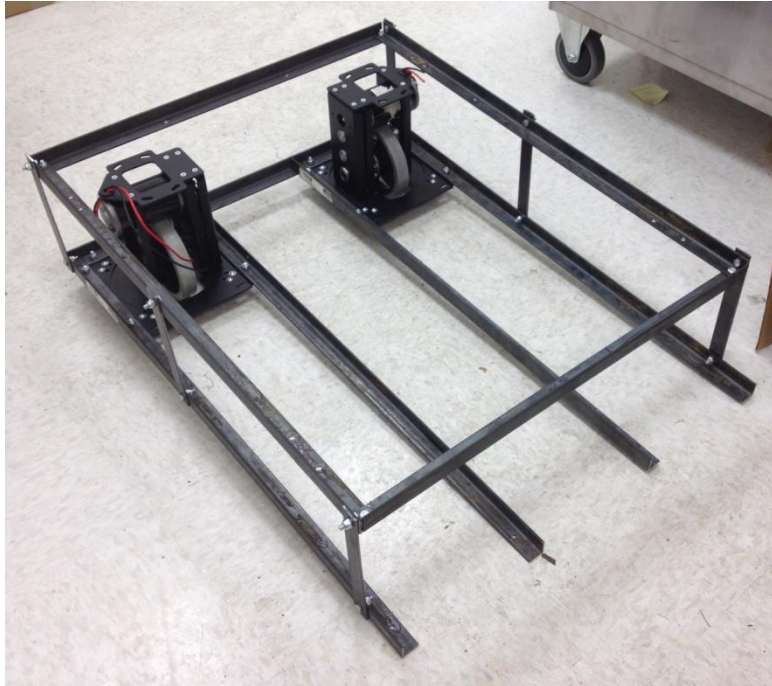


Figure 30: Partial frame during assembly

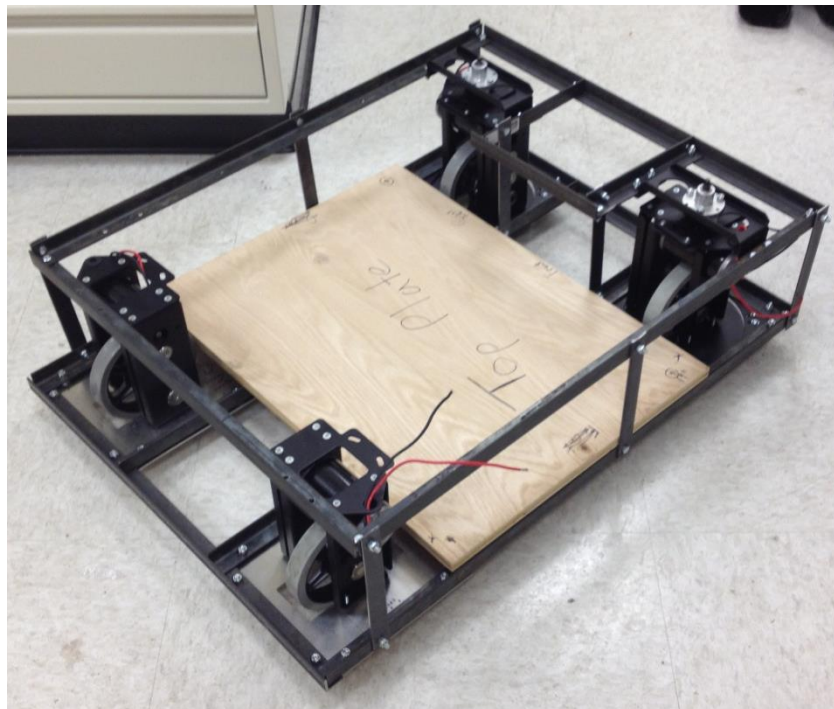


Figure 31: Completed frame with wheel modules

The completed frame consists of 12 pieces of the angle bar and additional pieces of flat 1/8" thick steel for vertical support. All four wheel modules are solidly attached at the top and bottom. To

ensure that all the bars were straight and at the appropriate level, we added washers as spacers between some of the pieces. We also positioned the upper plywood plate such that the sprockets for the steering assembly would line up vertically with the sprockets on the wheel modules. Although they are not shown in this picture, we also later added more of the flat steel bars on the sides of the frame to form a truss for additional rigidity.

Front Wheel Modules

Since we used off-the-shelf wheel modules, we saved a good amount of time in this regard, still, there were modifications that we had to make in order to use the AndyMark Wild Swerve units with our system. As discussed in the Project Design section, the main modification was using a different sprocket on top of the modules.

We began the process by following the kit's instructions to assemble the majority of the modules. Where we had to do the major work was at the end when we attached the sprocket to the bracket on top. The first thing we did was machine a keyway in the vertical bolt that runs through the whole top assembly. This was matched up with the existing keyway in the 22 tooth sprocket. We assembled this part of the module and finished attaching it to the chassis.

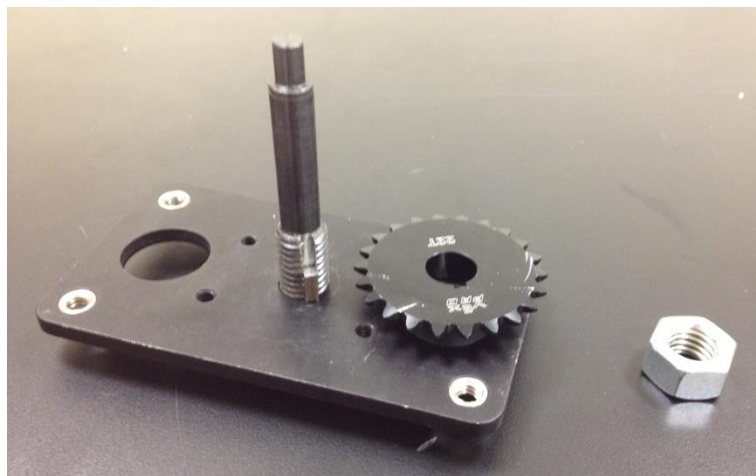


Figure 32: Sprocket assembly components

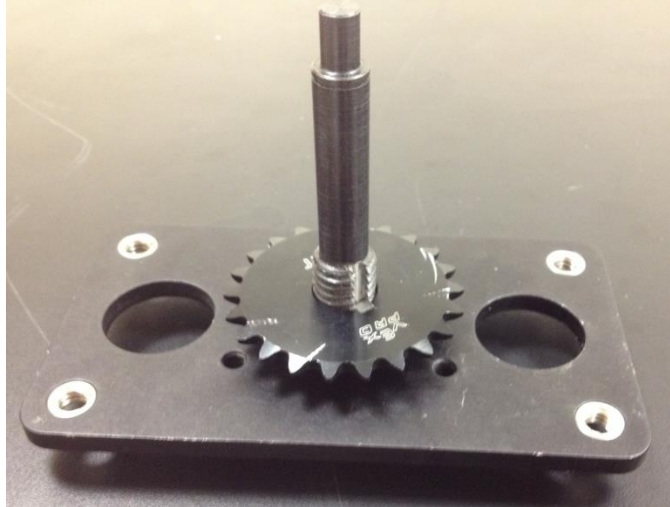


Figure 33: Modified sprocket assembly

We later found that the keyway was too loose, and allowed the wheel modules to rotate slightly even through the sprocket remained in place. We decided that the amount of play was enough that it could cause problems, particularly at high speed. To solve the problem, we removed the sprocket assemblies and added threaded holes through both the sprocket and the plate below it. By using four screws to directly hold the sprocket to the plate, we eliminated the wheel play entirely. Below is a picture of the completed top part of the module after it was attached to the robot, with the chain in place.



Figure 34: Completed assembly in place

Rear Wheel Modules

To save time, we used the same kits as the front wheel modules. We were able to purchase partial kits from AndyMark that did not come with the hardware that allows the modules to rotate. Unfortunately, some of the components were out of stock, so we had to machine our own shaft for one of the wheels. This part is shown in Figure 35. We made this part on the manual lathe out of 1/2" aluminum hex stock.

Additionally, we made replacements for the bottom plates as discussed in the Project Design section. These are made from a 1/8" thick aluminum sheet with appropriately sized holes drilled in it. The large cutout in the middle (for the wheel to fit through) was done with an end mill. As with the rest of the frame, this assembly was attached using 1/4-20 bolts and Nyloc nuts. We also added washers as spacers to ensure that both the front and rear wheels were level. The finished assembly for the rear wheels is shown in Figure 36.

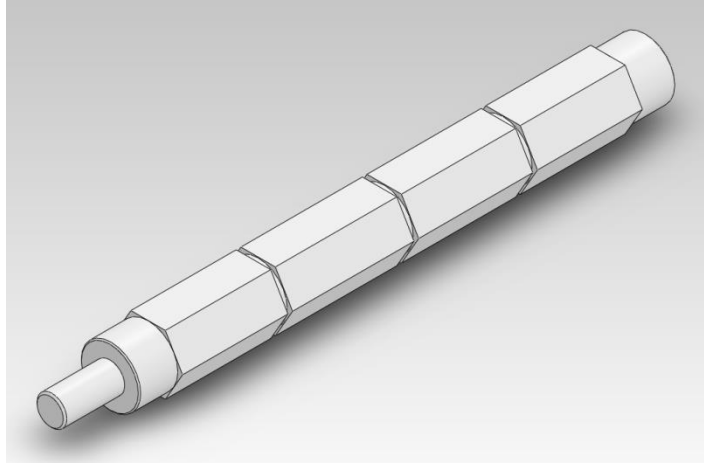


Figure 35: CAD for wheel shaft

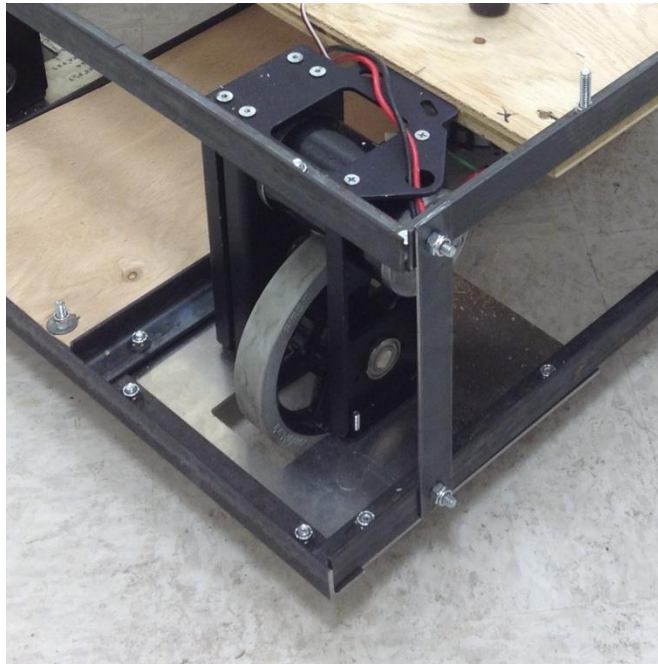


Figure 36: Completed rear wheel assembly

Steering Assembly

The construction and assembly was a fairly simple task which the most difficult part of was making sure dimensions were correct when machining. The first step in manufacturing the steering assembly was the creation of the linkages and the steering arm. The linkages and steering arm were created using aluminum 6061 bars. The bars were cut to size in a horizontal band saw and holes were added using the drill press. The hole dimensions are determined from the calculations done in the design section. It is important that the distance between these holes for the linkages are as accurate as

possible as errors in the dimensions will cause the steering system to operate improperly. A slot was also added in the steering arm for the pin-in-slot connection to the center links. To create the pin, a 1/4-20 bolt was inserted with nylon shaft around it to ensure the connection to the steering arm slot is tight yet the friction is still minimal.



Figure 37: Tie rod (top) and steering arm (bottom)

The sprockets we used for the steering assembly were purchased from VEXpro with the exception of the sprocket connected to the Bosch Van Door motor which was purchased from McMaster. 66-tooth aluminum sprockets for use with ANSI #25 chain were used for the larger part of the amplification system. The large sprocket connected to the steering arm was a 60-tooth aluminum sprocket for #35 chain. The choice was made to use the bigger chain because the forces generated by the Van Door motor were much higher than the forces the amplification chains would be receiving. Therefore #35 chain was used because the #25 would have been extremely close to receiving its maximum loading. Aluminum hubs purchased from AndyMark were connected to each of these plate sprockets. The steel 10-tooth sprocket for the Van Door motor had a built in hub and we connected it to the motor shaft using a keyed joint and a set screw to maintain its vertical position. Slots were placed in the three aluminum sprockets and a small slot was also added to links connected to these sprockets so that the sprockets could be shifted for alignment purposes. This process was suitable for the front sprockets but, this did not work with the steering arm sprocket. The large forces that occur at the extremes of the linkage system would cause the bolt in the connection between the steering arm and the sprocket to shift to the end of the slot in the sprocket. Because we were unable to obtain the resources to make this connection more solid, we drilled a single hole into the sprocket so the shifting would not occur.

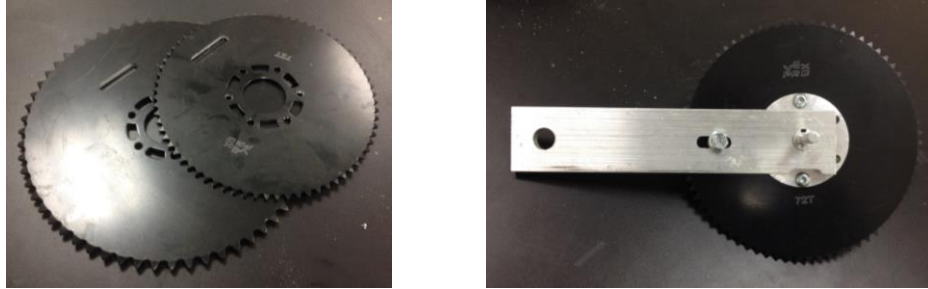


Figure 38: Plate sprockets with slots (left) and tie rod/sprocket assembly (right)

The steering assembly is all mounted to a plywood base which is fixed to the chassis. A more suitable option would have been to have some form of metal plate to mount everything to, but due to budget constraints and the ease of working with it, we chose to use plywood. First, bronze bushings were press fitted into the plywood based on the dimensions of our design. The steering assembly can be assembled separately with the links, sprockets, hubs, and shafts and then can be inserted into the bushings. The shafts were machined in the lathe out of aluminum and the tie rods were connected to center links using clevis pins. In our initial design, the top polycarbonate plate which would hold the upper bushings was to be 2 inches above the wooden plate. However, scrap aluminum blocks were found and to save on costs we chose to use them but the new polycarbonate plate would be 3 inches high.

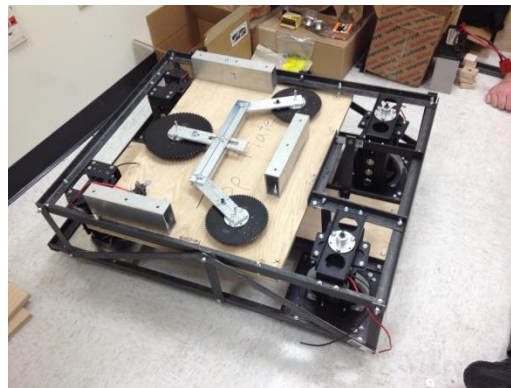


Figure 39: Manufactured steering assembly with standoffs

The change in the height of the top plate meant that other changes needed to be done. The polycarbonate was not sturdy enough hold the top bushings so the bushings needed to be mounted to small plywood pieces which could then be mounted to the polycarbonate. These bushings then needed to be lowered to minimize the bending forces on the shafts. The bending force on the shaft of the steering arm proved to be too much so a sturdier solution was needed. We replaced the aluminum shaft

with a steel shaft and mounted the upper bushing to a new steel support. With the change of material, the bending forces created by the Van Door motor were no longer a problem.

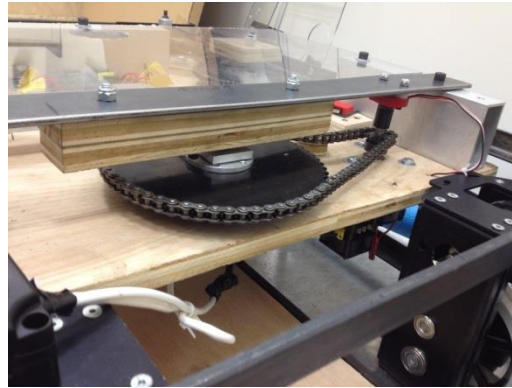


Figure 40: New steering arm assembly

The Van Door motor was mounted underneath the plywood base and the motor shaft comes up through the base so the 10t sprocket can be mounted directly to the shaft. The final mechanical assembly can be seen in Figure 41 which shows the completed robot along with bumpers added for safety.

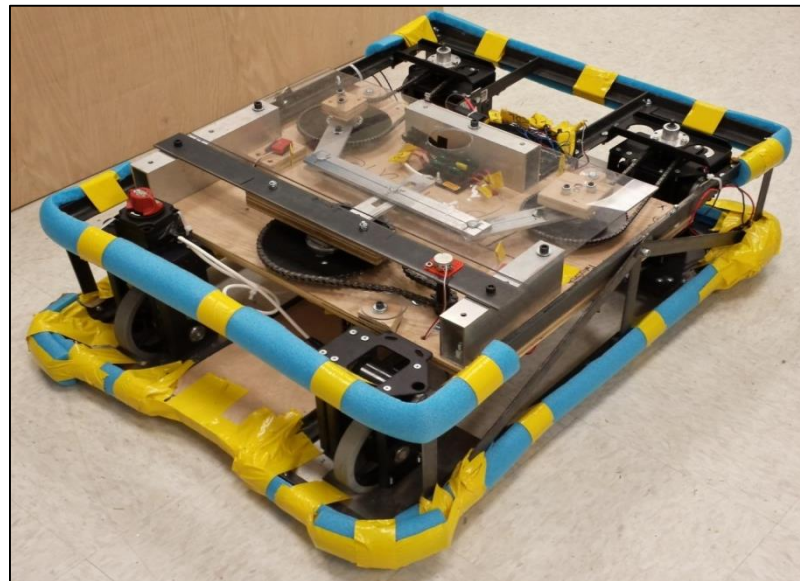


Figure 41: Completed robot driveline and chassis

Before operating the robot, an initial alignment must be performed. The wheels and the steering arm can be placed in a center position by loosening the bolts connecting the links to the sprockets. Once the steering assembly is aligned, it can be set into position by retightening the bolts and

setting up the tensioners on the chain. The tensioners were made using 1/8th inch thick polycarbonate discs and a small plywood block held to the base with a single bolt. By pressing the disc to the chain, we can maintain a tight connection during the operation of the robot.

Electrical Assembly

The electrical systems of our robot consist of an Arduino mega 2560 microprocessor and board, a Turnigy 9x receiver and transmitter, an ATC fuse block, a standard 12v battery, two VEX bump sensors, 5 victor speed controllers and a 300° potentiometer. We used 22 gauge wire to go from the Arduino to the Victor speed controllers since they would never exceed five volts and one amp. To wire from the battery to the CIM and Van Door motors we used 10 gauge wires, because we wanted to prepare for the CIM motors to draw as much as 40 amps which would be regulated via our fuse block, although if left unchecked they could pull as many as 130 amps. In order to protect the sensors, motors, and Arduino we wired all of our components through an ATC fuse block. The block itself was only able to withstand 30 Amps, which was not ideal as we wanted the CIM motors to draw up to 40 amps and over the course of testing we found that we frequently had to replace these fuses.

We chose the Arduino Mega 2560 microcontroller to handle all of the programming for our system for several reasons. It's a very inexpensive and reliable system, with extensive open source code libraries that we were able to make use of. The Mega 2560 also has additional FLASH and RAM memory, which was an initial concern before we knew how intensive our wheel speed equations would be. Finally, the Mega 2560 has additional serial ports, timers, and I/O pins. We mounted this to the front of our robot outside the polycarbonate top, so that we could easily access it. We also drilled holes on either side of the Arduino so that we could run wires under the plywood. This allowed us to better organize the wires and ensure they did not become entangled in any moving parts.

The Turnigy 9x is a standard remote control for hobbyist airplane and helicopters. For this piece of equipment the requirements were that it operates on a public band, that it had a range of at least 50 yards, and had at least two channels for forward/reverse and turning left/right. This remote was able to easily meet all of these requirements and was a very economic option for us, and therefore we opted to make use of it. We mounted the receiver to our chassis with zip ties near the Arduino so that we would be able to easily wire the two together. We used two channels, 2 and 4, from the remote control simply

because it was easier to wire if we did not use channels that were immediately adjacent to each other. These were wired into pins 5 and 6 on the Arduino.

The ATC fuse block was a six fuse one, with a maximum rating of 30 amps. Unfortunately we were unable to find one that was rated for 40 amps, which was our only real requirement for the block. Because of this we went with 30 amp ATC fuses to try to ensure we did not damage the block or any other systems. The 12v battery we wired directly to the fuse block and to a separate block we used as a common ground for all the systems on the chassis.

We ended up deciding to use three sensors on our system to provide control to a driver. One was a 300° potentiometer which we mounted to the van door motor via a 3D printed adapter, this can be seen in Figure 42. We centered the potentiometer so it read 511 when the wheels were aligned and used this to determine how far to the left or right the wheels would be turned. We would map the range of the joystick on the controller to the range for the potentiometer to make either a full left or right turn. We would then use a PID loop to move the turning motor until it reached the value being sent by the remote. The other two sensors on the robot were VEX bump sensors mounted so that when our tie rod got to the extremes of its range of motion it wouldn't push past its limits and lock up. All of these sensors had holes drilled into the plywood not far from where they were mounted and their cables were run through them and to the Arduino. We put the potentiometer into analog pin 0, and we used pins 2 and 3 for the bump sensors. Initially we chose pins 2 and 3 for the bump sensors because those pins have interrupts on them, and we intended to use interrupts to stop the turning motor when the bump sensors were depressed. Eventually in the implementation we found that rather than using the interrupt, performing a check when trying to turn either direction to see if the button was depressed allowed for a more elegant solution.

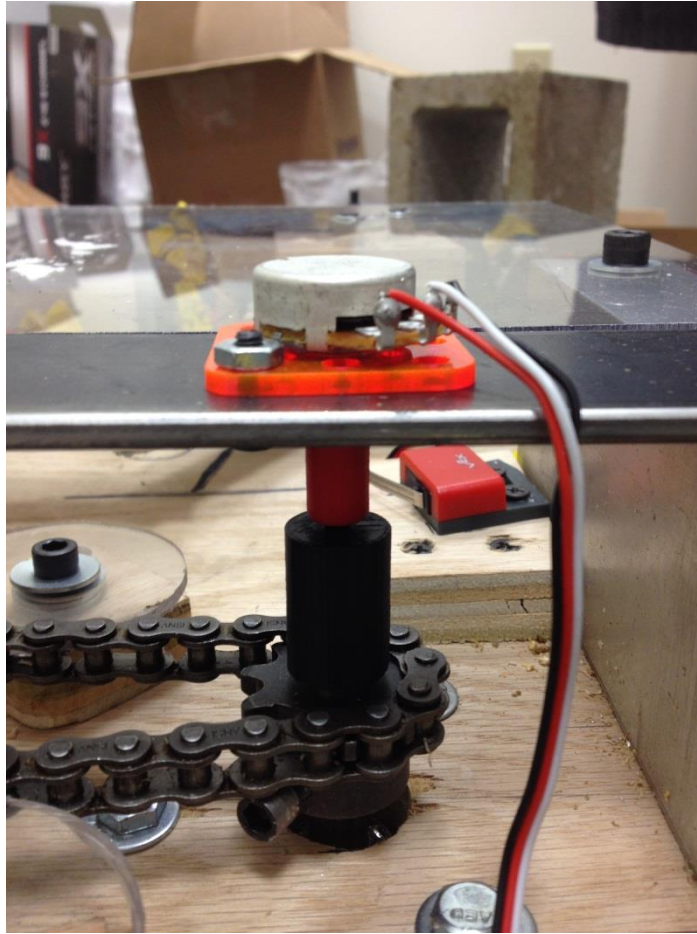


Figure 42: A picture of our potentiometer with the 3D printed adapter to the turning motor.

Programming Implementation

Attached in Appendix B is the entire code that we used for our robot. Arduinos operate through two main function calls, the first of these being setup and the next being loop. Setup, just like its name alludes to, is where everything is initialized before the loop function. The loop function goes through all the code that is inside it as long as the board is powered. Loop will contain the code that is listening to the sensors and controller and then making changes based upon what input it receives from them. When there is a change from one of the various inputs, the values are sent to the appropriate functions for calculations and necessary changes. Constants were used on all variables that should never be changed, such as the names that were given for particular pins or definitive speeds such as stop. Doubles were used for every other value due to increased accuracy and the use of decimal values that was necessary to ensure that our equations were accurate. Things of note with our code are that we

send the desired speed of the wheels as servo values using the Arduino servo library. The reason for this is that the Victors are able to convert this servo value to a standard PWM and thus saves us the trouble of needing to do it ourselves. Below you can find the wheel speed algorithm we used in our code to determine each individual wheel speed. Theta (θ) represents the degree of turn in relation to the front outer wheel; the potentiometer value is used for this. Also shown below is a graph of the velocity of each of the four wheels depending on the current steer angle.

$$velocityFrontOuter = throttle\ input$$

$$radiusFrontOuter = \frac{wheelBase}{\cos\left(\frac{\pi}{2}\right) - \theta}$$

$$\omega = \frac{velocityFrontOuter}{radiusFrontOuter}$$

$$radiusRearOuter = \sqrt{radiusFrontOuter^2 - wheelBase^2}$$

$$radiusRearInner = |radiusRearOuter - wheelTrack|$$

$$radiusFrontInner = \sqrt{wheelBase^2 + radiusRearInner^2}$$

$$velocityFrontInner = \omega * radiusFrontInner$$

$$velocityRearInner = \omega * radiusRearInner$$

$$velocityRearOuter = \omega * radiusRearOuter$$

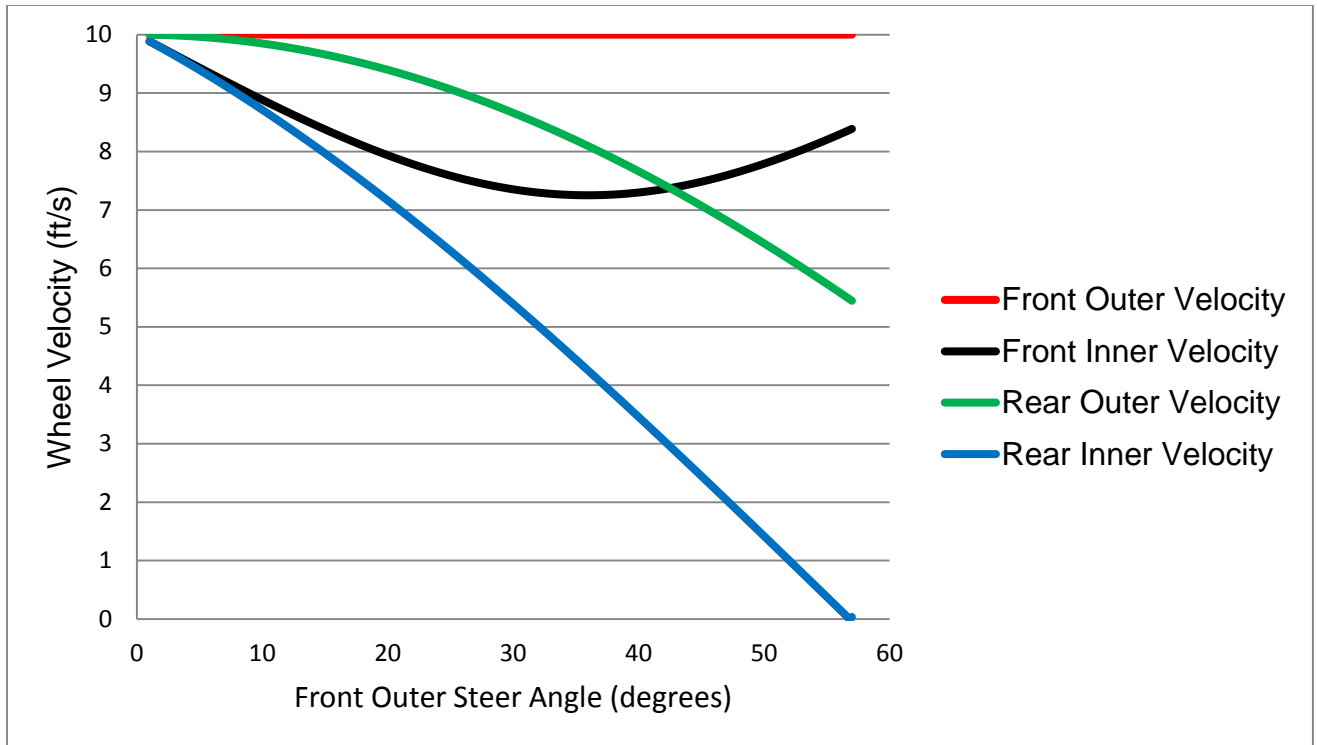


Figure 43: Wheel velocity vs. steer angle

This code takes the throttle input from the controller and potentiometer value. From these inputs and the wheel track and wheel base measurements, we can calculate the speed that each wheel needs to spin to make a given turn. Wheel track is essentially the width, measured from the center of one wheel to the center of the other wheel directly across from it. Wheel base is the length which is measured from the center of one wheel to the center of the wheel directly in line with it.

Testing and Evaluation

Individual Performance Evaluation

To test our driveline, we were first able to determine its zero radius turning capability, the ability of the driveline to maintain the 10-foot radius circle, and overall handling and performance. These evaluations can be done without the need of another robot for comparison. For the circle test, we drove the robot on a carpeted surface like that which is typically used for FRC competitions. Due to space limitations and lack of carpet, we were unable to test the 10-foot radius circle capabilities. However, we were able to test using a 5-foot radius instead. The tighter radius is actually more difficult to achieve, so the robot should still be capable of the same performance assuming that there was enough space and the same surface was used. The results of this test are detailed below.

Comparative Performance Evaluation

For the comparative performance evaluation, we created a test course and assembled a team of drivers to race both our robot and the robot from FRC Team 190's 2013 competition. Team 190's 2013 robot is a 6 wheel tank drive driveline with omni wheels in the rear. It uses four CIM motors for driving the wheels and is nearly identical size and weight to our own driveline making it a great candidate for comparison considering it uses one of the most common drivelines for FRC robots. We added additional weights on the bottom platform of our robot so that the two robots had the same weight.

As for the course, it was created by adding modified elements of the standard Emergency Vehicle Operations Course (EVOC). These course elements ensure that we can examine different aspects of vehicle performance. Figure 44 shows the course we designed.

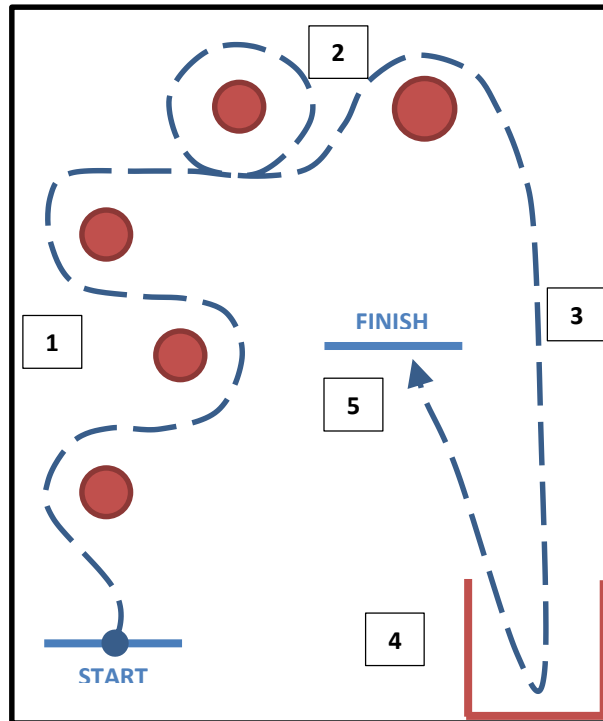


Figure 44: Performance course

The first element of this course is the serpentine to test high speed turning capabilities of the robot. Next is a figure eight maneuver which tests even smaller radius turning. Third is a straight line which tests the robot's ability to accelerate out of a turn and maintain a straight path. Fourth is a confined space 180° turn. This element tests the low speed maneuverability of the robot. Theoretically, the FRC robot should outperform us in this area as it can turn about the center point of its chassis. Finally, a straight line to the finish is the last step. This course was assembled using cones as markers for the obstacles. We decided that hitting a cone would result in a 5 second deduction. Comparing the times of both robots on this course would give us good feedback regarding the performance of our robot using the FRC robot as a baseline. As for the drivers for this test, we were able to enlist the help of nine test drivers. Six drivers had previous FRC driving experience while the other three had no robot driving experience whatsoever. This mix of driver experience would allow us to get quantitative and qualitative feedback from drivers with varying backgrounds. To conduct the test, we had all nine drivers complete a run using one of the robots and the times for each driver were recorded including the number of obstacles hit. To measure energy efficiency, the battery voltage was measured before and after all nine drivers had completed one run.

Conclusion

Results

As was predicted, the driveline is capable of zero radius turning about either of the back wheels. When the wheels are turned to the zero radius condition, the robot can rotate seamlessly in either direction by applying forward or reverse throttle. This test shows that we were able to achieve the zero radius turning goal by turning about a point within the chassis.

The results from the circular driving test showed that the robot was able to maintain the 4-foot driving lane at full throttle, accomplishing one of our goals for high speed stability. While we had some difficulty in maintaining the correct steer angle so that the robot stayed exactly on the circle, we were able to make enough consecutive circles to average the times and determine that the speed had reached 10 ft/sec.

Figure 45 shows the average course times for each driver for both the FRC robot and the MQP robot. Non-experienced drivers are denoted by the initials NE. The recorded driver times from this test can be found in appendix A. Unfortunately, the FRC robot had better times than the MQP robot. Without deductions for hitting obstacles, the FRC robot was 1.8% faster than the MQP robot. However, our robot hit 2.4 times as many obstacles as the FRC robot. On a per driver basis, course times with the MQP robot improved by 7.5 seconds more than the FRC robot on average. This shows that although the FRC robot had better performance times, drivers were beginning to adapt to the controls of the MQP robot and with more time may have been able to surpass the performance times of the FRC robot.

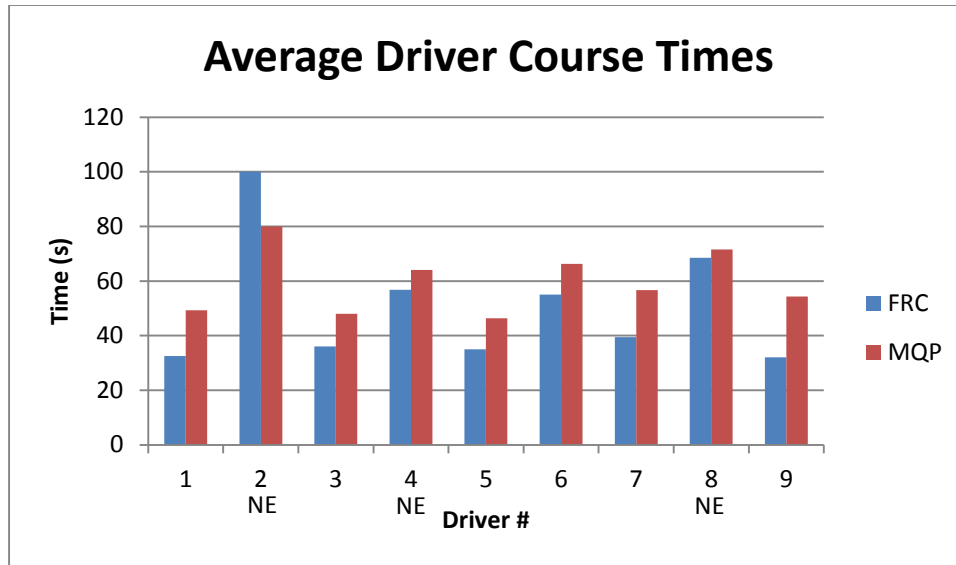


Figure 45: Average driver course times

Despite the quantitative results showing deficiencies in our driveline, the qualitative feedback and our own observations provided a lot of useful information. The general consensus from the drivers was that our controls were too sensitive. Drivers had trouble maintaining a straight line and would tend to swerve as they overcorrected the steering. Some said a different controller choice might solve that issue while one driver also said that if the spring in the joysticks was simply stronger, then that would have been much better as well. Although drivers were unhappy with the sensitivity, they were very happy with the mechanical capabilities of the robot as well as the intuitiveness of the controls. The non-experienced drivers also said that our robot was much easier to quickly understand.

In terms of energy efficiency, the MQP robot was much more efficient. The MQP robot was anywhere from 2.5 to 8.5 times more energy efficient than the FRC tank drive robot. The average voltage loss of the FRC robot was 1.26 volts while the MQP robot's average voltage loss was 0.315 volts resulting in our robot being four times more energy efficient than the FRC robot on average. In order to complete all nine runs of the test, the FRC robot's battery even needed to be changed due to voltage loss in order to be driven effectively.

Discussion

Our own impressions of the robot's performance were very good. Driving the robot was intuitive as the controls were simple and the handling was relatable to the standard automobile. However, the

controller's joysticks were very sensitive and it made mid steer angles hard to maintain. Adjustments were made to the programming to try and make those ranges less sensitive. While these changes helped, the controller itself just seemed too sensitive to begin with. With our own performance tests, we found that the robot handled very well despite these sensitivity issues and was even capable of going from full throttle forward motion to a full throttle zero radius turn with minimal skidding due to its forward momentum. All of these tests were very promising for future use of this driveline design.

From our observations, we noted that nearly all drivers had a hard time understanding the zero radius turning capabilities that our robot provided. Especially in the confined space turn, drivers would have the wheels in the correct full turn and simply accelerate in the wrong direction or turn the wrong way. Our reasoning was that because the operation of our robot was so similar to that of a common automobile, the drivers had a harder time adapting to the increased range of motion. Based on all of the feedback we received, we are very confident that the MQP robot times would beat the FRC times if the sensitivity of the controls was improved upon and drivers were given more time to learn the capabilities of our driveline.

In particular, the ability of our robot to execute smooth turns and drive in a uniform circle is very beneficial. This capability is something that most FRC robots cannot achieve, especially tank drive. We could see that during the serpentine section of the course, drivers quickly learned how to make gradual turns which cut down on time. The skid steered FRC robot tended to stop after each cone and adjust their angle before continuing.

Another major advantage that our system has is the increased energy efficiency. While this advantage to our robot was expected, the degree to which it occurred was surprising. The inherent skid steering of the tank drive robot was the source of the high inefficiency. The FRC robot's battery even had to be changed in order to effectively complete a run with all nine drivers.

The significant improvements that could stand to be made to our design are in the overall size of our mechanism, the method of driving the tie rod that controls wheel turning, and finally the user interface. Each of these were designed and built adequately to meet our goals, but could still be better designed to make for easier use on other systems.

The pin-in-slot system that we used to drive our linkage required both a large amount of torque to drive at its extreme ranges as well as using up a large portion of the top of the chassis. In order to make the chassis better able to support additional manipulators and equipment, the system should

ideally be made more compact. We suspect that if the equations we developed to find the proper turn angles were applied to a smaller linkage system, this space could be reduced. Similarly, our pin-in-slot method of driving the tie rod needed a very large amount of torque to be able to properly position the wheels when they got close to their extreme ranges. We believe that there is likely a solution for this that one could create with linkages that would generate the same motion, but require much less torque at its extremes as well as helping to prevent the problem of the linkages locking up at their extremes. By changing the pin-in-slot, additional space behind the linkage could be created.

Depending on the application of the robot, having the turning point between the two rear wheels might be a better choice. We chose to turn about one of the rear wheels for simplicity and because our linkage would lock up shortly after that. However, if the linkage were modified and actuated using a different system, the wheels could turn even farther to allow the robot to turn about a point at the center of the rear axle.

The control system we chose was to use was that of a hobby RC airplane remote. The y axis on the left joystick was used as throttle, and the x axis of the right joystick was used for turning. This system was chosen in major part for its simplicity and the inexpensiveness of the controller itself. Unfortunately the range of motion of the controller was not as large as we would have liked and we quickly saw that people tended to drive at the extremes of the turning range, rather than making use of the middle ranges. We believe it to be possible to rectify this problem in several ways. One option would be to use a different controller altogether, such as a hobby RC car remote with a small wheel on it that would be used for steering, and a simple trigger for throttle. Another potential option is to simply choose a remote control that gives more force-feedback as you increase the turn range, that way the user gets more feedback about how far they're driving the turning mechanism and they are less likely to use its extremes when they don't need to.

Social Implications

After completing our prototype, we believe that it could certainly be used for a wide variety of applications. Any vehicle that is required to operate at high speed as well as make tight turns could benefit from a system like the one we developed. This includes certain robots, as well as street cars, trucks, construction equipment, tractors, lawn mowers, and recreational vehicles.

For applications that currently use Ackermann steering, like cars, the impact of our system would be most significant. It would allow these vehicles to be more maneuverable in confined spaces

and perform precise maneuvers with greater speed and ease. One result of this would be that travel times would be reduced. This would directly make a difference in many peoples' lives, but could also allow emergency vehicles and law enforcement to reach locations faster. Another result of the increased maneuverability compared to Ackermann is that some infrastructure could be made more space efficient. Many of the systems that are currently optimized for typical cars, such as intersections, parking lots, and garages, could potentially be made smaller.

Another result of using our system over drivelines that are currently used for low speed maneuverability is the increased efficiency. Energy could be saved in applications that currently involve tank drive or mecanum drive. While these systems are relatively uncommon, they are so inefficient that replacing them could have a great impact by reducing fuel costs for those who do use them. Over the long term, this could also slightly reduce harmful emissions and cut down on the usage of nonrenewable fuel sources.

The ability to perform a turn in place may open up new possibilities for slow moving construction and farm equipment as well. If large, heavy machines were able to maneuver themselves into tight spaces more easily and reach positions that are not currently feasible, it may be possible to reduce construction timelines and generally increase productivity wherever these vehicles are used. In some situations, this may even reduce the cost of certain goods and services for consumers.

Final Conclusions

Our design was mechanically a very viable option for future use in either FIRST robotics or potentially for larger vehicles that need more maneuverability than standard Ackermann can provide. It was able to meet all of the specifications we set out for it, with the sole exception of being faster than the FRC Team 190 robot. We believe based on the driver feedback and results of our tests, however, that this loss was not due to a mechanical failure of our system, but rather that it was due to an underdeveloped user interface system. The goals that it was able to accomplish are: reach a speed of at least 10ft/s, maintain a 4 foot lane while driving a 10 foot radius circle, and be able to turn about a point within the perimeter of the chassis. Some more general goals that we tried to optimize for were to maximize traction at low speeds by powering each wheel independently, to maximize the energy efficiency of the system by reducing skidding, limit the degrees of freedom of the system, and finally to comply with all the FRC rules of the 2013 season. Since we met each of these desired goals with the one

exception, the design was a success as a proof of concept. After future improvements, we feel it could be useful in a very wide variety of applications.

Appendices

Appendix A: Driver performance course data

SPEED TEST	Driver 1			Driver 2 (NE)			Driver 3			Driver 4 (NE)		
	Time	Deductions	Adj. Time	Time	Deductions	Adj. Time	Time	Deductions	Adj. Time	Time	Deductions	Adj. Time
Run 1 (FRC)	28	5	33	75	25	100	41	0	41	63.5	5	68.5
Run 2 (MQP)	36.5	10	46.5	65	15	80	39	5	44	60	15	75
Run 3 (FRC)	27	5	32				31	0	31	45	0	45
Run 4 (MQP)	32	20	52				41	10	51	43	10	53
Run 5 (MQP)							24	25	49			

SPEED TEST	Driver 5			Driver 6			Driver 7			Driver 8 (NE)			Driver 9		
	Time	Deductions	Adj. Time	Time	Deductions	Adj. Time	Time	Deductions	Adj. Time	Time	Deductions	Adj. Time	Time	Deductions	Adj. Time
Run 1 (FRC)	36	5	41	60	5	65	36	5	41	68	10	78	31	5	36
Run 2 (MQP)	43	10	53	73	30	103	43	25	68	55	25	80	41	10	51
Run 3 (FRC)	29	0	29	35	10	45	28	10	38	44	15	59	28	0	28
Run 4 (MQP)	36	5	41	35	10	45	36	15	51	38	25	63	55	10	65
Run 5 (MQP)	25	20	45	31	20	51	36	15	51				42	5	47

Appendix B: Code

```
/* Optimal Driveline MQP */
```

```
// Variables and Values associated with the Victors
```

```
#include <Servo.h>
```

```
#include <Math.h>
```

```
// wheels are determined by looking down at the top of the robot with the front of the robot facing up
```

```
#define VICTOR_FL 22 // the pin that the victor's signal line is attached to Front Left
```

```
#define VICTOR_FR 33 // the pin that the victor's signal line is attached to Front Right
```

```
#define VICTOR_RL 8 // the pin that the victor's signal line is attached to Rear Left
```

```
#define VICTOR_RR 35 // the pin that the victor's signal line is attached to Rear Right
```

```
#define VICTOR_VD 37 // the pin that the victor's signal line is attached to Van Door
```

```
Servo victorFL;
```

```
Servo victorFR;
```

```
Servo victorRL;
```

```
Servo victorRR;
```

```
Servo victorVD;
```

```
int const fullStop = 1500; // Servo values are used
```

```

int const fullForward = 2000; // Servo values are used
int const fullReverse = 1000; // Servo values are used
double frontOuter;
double frontInner;
double rearInner;
double rearOuter;

//Turning values
double desVal;
double curVal;
double turnSpeed;
double additionalSpeed;

// Variables and Values associated with the Turning Equations
// wheelBase and wheelTrack need to be measured
// not sure what units to be used for these measurements
double const wheelBase = 26;
double const wheelTrack = 17;
double velocityFrontOuter;
double radiusFrontOuter;
double omega;
double radiusRearOuter;
double radiusRearInner;
double radiusFrontInner;
double velocityFrontInner;
double velocityRearInner;
double velocityRearOuter;

// Variables and Values associated with the Potentiometer
const int potPin = A0;
double potIn = 0;

// Variables and Values associated with the Tx/Rx
int const throttlePin = 5; // ch2
double throttleCh;
int const turnPin = 6; // ch4
double turnCh;
double throttleOut;
double turnOut;

// Variables and Values associated with the Limit Switches
int const leftLimitPin = 2;
int const rightLimitPin = 3;
int leftBump;
int rightBump;

void setup() {
  // Initialize Serial

```

```

Serial.begin(9600);

// Setup for Tx/Rx
pinMode(throttlePin, INPUT);
pinMode(turnPin, INPUT);

// Setup for Victors
victorFL.attach(VICTOR_FL);
victorFR.attach(VICTOR_FR);
victorRL.attach(VICTOR_RL);
victorRR.attach(VICTOR_RR);
victorVD.attach(VICTOR_VD);

// Setup for Limit Switches
pinMode(leftLimitPin, INPUT_PULLUP);
pinMode(rightLimitPin, INPUT_PULLUP);
}

void loop() {
  // Tx/Rx Code
  // Read the signals from the channels
  throttleCh = pulseIn(throttlePin, HIGH, 25000);
  turnCh = pulseIn(turnPin, HIGH, 25000);

  // converts the controller input to servo values
  throttleOut = map(throttleCh, 1015, 1880, 1000, 2000);
  turnOut = map(turnCh, 1015, 1880, 1000, 2000);
  //Serial.print("Throttle Out:");
  //Serial.println(throttleOut);
  //Serial.print("Turn Out:");
  //Serial.println(turnOut);
  //delay(100);

  // Potentiometer Code
  potIn = analogRead(potPin); // reads sensor value
  Serial.print("potIn Value Is:");
  Serial.println(potIn);

  //Bump Sensor
  leftBump = digitalRead(leftLimitPin);
  rightBump = digitalRead(rightLimitPin);
  //Serial.print("Left Limit is:");
  //Serial.println(leftBump);
  //Serial.print("Right Limit is:");
  //Serial.println(rightBump);

  // Turning Code
  turnCompute();
}

```

```

// testing code
/*if (throttleOut > 1700){
  victorFR.writeMicroseconds(1800);
  victorFL.writeMicroseconds(1800);
  victorRR.writeMicroseconds(1800);
  victorRL.writeMicroseconds(1800);
  Serial.print("throttleCh:");
  Serial.println(throttleCh);
  Serial.print("throttleOut:");
  Serial.print(throttleOut);
}
else if (throttleOut < 1300){
  victorFR.writeMicroseconds(1200);
  victorFL.writeMicroseconds(1200);
  victorRR.writeMicroseconds(1200);
  victorRL.writeMicroseconds(1200);
  Serial.print("throttleCh:");
  Serial.println(throttleCh);
  Serial.print("throttleOut:");
  Serial.print(throttleOut);
}
else {
  victorFR.writeMicroseconds(fullStop);
  victorFL.writeMicroseconds(fullStop);
  victorRR.writeMicroseconds(fullStop);
  victorRL.writeMicroseconds(fullStop);
}*/

// Forward Driving
// throttleCh and throttleOut are interchangeable, just remember to use servo values instead
if (turnOut > 1450 && turnOut < 1550) { // Driving Straight
  if (throttleOut > 1550) { // Forward
    victorFR.writeMicroseconds(invertSpeed(throttleOut));
    victorFL.writeMicroseconds(throttleOut);
    victorRR.writeMicroseconds(invertSpeed(throttleOut));
    victorRL.writeMicroseconds(throttleOut);
    // Serial.print("Forward");
    // Serial.print("\n");
    /*Serial.print("victorFR:");
    Serial.println(throttleOut);
    Serial.print("victorFL:");
    Serial.println(throttleOut);
    Serial.print("victorRR:");
    Serial.println(throttleOut);
    Serial.print("victorRL:");
    Serial.println(throttleOut);*/
  }
}

```

```

else if (throttleOut < 1450) { // Reverse
  victorFR.writeMicroseconds(invertSpeed(throttleOut));
  victorFL.writeMicroseconds(throttleOut);
  victorRR.writeMicroseconds(invertSpeed(throttleOut));
  victorRL.writeMicroseconds(throttleOut);
  // Serial.print("Reverse");
  // Serial.print("\n");
  /* Serial.print("victorFR:");
  Serial.println(throttleOut);
  Serial.print("victorFL:");
  Serial.println(throttleOut);
  Serial.print("victorRR:");
  Serial.println(throttleOut);
  Serial.print("victorRL:");
  Serial.println(throttleOut);*/
}
else {
  victorFL.writeMicroseconds(fullStop);
  victorFR.writeMicroseconds(fullStop);
  victorRL.writeMicroseconds(fullStop);
  victorRR.writeMicroseconds(fullStop);
}
}
else if (turnOut < 1450 && throttleOut > 1550) { // Forward Left Turn
  speedCompute();
  victorFR.writeMicroseconds(invertSpeed(velocityFrontOuter));
  victorFL.writeMicroseconds(velocityFrontInner);
  victorRR.writeMicroseconds(invertSpeed(velocityRearOuter));
  victorRL.writeMicroseconds(velocityRearInner);
  /*Serial.print("Left Turn Forward");
  Serial.print("\n");
  Serial.print("victorFR:");
  Serial.println(velocityFrontOuter);
  Serial.print("victorFL:");
  Serial.println(velocityFrontInner);
  Serial.print("victorRR:");
  Serial.println(velocityRearOuter);
  Serial.print("victorRL:");
  Serial.println(velocityRearInner);*/
}
else if (turnOut > 1550 && throttleOut > 1550) { // Forward Right Turn
  speedCompute();
  victorFR.writeMicroseconds(invertSpeed(velocityFrontInner));
  victorFL.writeMicroseconds(velocityFrontOuter);
  victorRR.writeMicroseconds(invertSpeed(velocityRearInner));
  victorRL.writeMicroseconds(velocityRearOuter);
  /*Serial.print("Right Turn Forward");
  Serial.print("\n");

```



```

Serial.print("victorFR:");
Serial.println(velocityFrontOuter);
Serial.print("victorFL:");
Serial.println(velocityFrontInner);
Serial.print("victorRR:");
Serial.println(velocityRearOuter);
Serial.print("victorRL:");
Serial.println(velocityRearInner);*/
}
else if (turnOut < 1450 && throttleOut < 1450) { // Reverse Left Turn
  speedCompute();
  victorFR.writeMicroseconds(invertSpeed(velocityFrontOuter));
  victorFL.writeMicroseconds(velocityFrontInner);
  victorRR.writeMicroseconds(invertSpeed(velocityRearOuter));
  victorRL.writeMicroseconds(velocityRearInner);
  /*Serial.print("Left Turn Reverse");
  Serial.print("\n");
  Serial.print("victorFR:");
  Serial.println(velocityFrontOuter);
  Serial.print("victorFL:");
  Serial.println(velocityFrontInner);
  Serial.print("victorRR:");
  Serial.println(velocityRearOuter);
  Serial.print("victorRL:");
  Serial.println(velocityRearInner);*/
}
else if (turnOut > 1550 && throttleOut < 1450) { // Reverse Right Turn
  speedCompute();
  victorFR.writeMicroseconds(invertSpeed(velocityFrontInner));
  victorFL.writeMicroseconds(velocityFrontOuter);
  victorRR.writeMicroseconds(invertSpeed(velocityRearInner));
  victorRL.writeMicroseconds(velocityRearOuter);
  /*Serial.print("Right Turn Reverse");
  Serial.print("\n");
  Serial.print("victorFR:");
  Serial.println(velocityFrontOuter);
  Serial.print("victorFL:");
  Serial.println(velocityFrontInner);
  Serial.print("victorRR:");
  Serial.println(velocityRearOuter);
  Serial.print("victorRL:");
  Serial.println(velocityRearInner);*/
}
else {
  victorFL.writeMicroseconds(fullStop);
  victorFR.writeMicroseconds(fullStop);
  victorRL.writeMicroseconds(fullStop);
  victorRR.writeMicroseconds(fullStop);
}

```

```

    /*victorVD.writeMicroseconds(fullStop);
    Serial.println("Stop");*/
}
} // End of void loop()

// Start of helper functions
int invertSpeed (int x) { // used to make sure all wheels are going right direction
    int y = 0;
    if (x > 1500) {
        y = 2000 - x;
        return 1000 + y;
    }
    if (x < 1500) {
        y = x - 1000;
        return 2000 - y;
    }
}

double potRadVal (double x) { // converts pot value to Radians to use with cos
    // 472.5 is dead center of 0-945 output
    // about 1 ticks for every degree of rotation
    // front wheels have a total movement of 147°
    // 0 to 90° if front inner
    // 0 to 57° if front outer
    // 0° is straight
    double y = 0;
    if (x > 513) {
        y = (x/8.275)-57;
        return y*(3.14/180); // converts from degrees to radians
    }
    else if (x < 431) {
        y = (-x/8.275)+57;
        return y*(3.14/180); // converts from degrees to radians
    }
    else {
        return 0;
    }
}

double stickToPot (double x) { // converts the turn stick input to Pot Values
    double y = 0;
    if (x <= 1450) { // left side of turn stick to pot values
        if (x >= 1060) { // between 30 degree and 0
            y = x*0.8-742;
            return y;
        }
        else { // greater than 30 degree
            y = x*1.7391-1737.5;

```

```

    return y;
}
}
else if (x >= 1550) { // right side of turn stick of pot values
    if (x <= 1940) { // between 30 degree and 0
        y = x*0.8-742;
        return y;
    }
    else { // greater than 30 degree
        y = x*1.7391-2563.9;
        return y;
    }
}
}
else {
    return 435; // theoretical center for pot
}
}

double voltageToServo (double x) {
    // convert from voltage to servo
    return x*38.5+1500;
}

double servoToVoltage (double x) {
    // convert from servo to voltage
    return (x/38.5)-38.5;
}

void speedCompute () {
    velocityFrontOuter = servoToVoltage(throttleOut);
    radiusFrontOuter = wheelBase/(cos((3.14/2)-potRadVal(potIn)));
    omega = velocityFrontOuter/radiusFrontOuter;
    radiusRearOuter = sqrt(pow(radiusFrontOuter,2)-pow(wheelBase,2));
    radiusRearInner = abs(radiusRearOuter-wheelTrack);
    radiusFrontInner = sqrt(pow(wheelBase,2)+pow(radiusRearInner,2));
    velocityFrontInner = omega*radiusFrontInner;
    velocityRearInner = omega*radiusRearInner;
    velocityRearOuter = omega*radiusRearOuter;
    velocityFrontOuter = voltageToServo(velocityFrontOuter);
    velocityFrontInner = voltageToServo(velocityFrontInner);
    velocityRearOuter = voltageToServo(velocityRearOuter);
    velocityRearInner = voltageToServo(velocityRearInner);
}

void turnCompute () {
    // Code to drive van door motor to desired position
    curVal = potIn/945; // set value of current pot position using range of 1000 to get % of turn
    desVal = stickToPot(turnOut)/945; // set value of desired position using % of turn
}

```

```

//Serial.print("potIn is:");
//Serial.println(potIn);
//Serial.println("Pot Degree Val");
//Serial.println(potRadVal(potIn));

if ((curVal - .025) <= desVal && (curVal + .025) >= desVal) {
  victorVD.writeMicroseconds(fullStop);
  //Serial.println("victorVD is stopped:");
  //Serial.println(turnCh);
}
if (curVal >= desVal && rightBump == 1) { //turn left
  additionalSpeed = (0.5 - desVal) * 800;
  turnSpeed = ((curVal - desVal) * 1000) + additionalSpeed;
  if (turnSpeed < 150) {
    turnSpeed = 150;
  }
  if (turnSpeed > 500) {
    turnSpeed = 500;
  }
  victorVD.writeMicroseconds(1500 - turnSpeed);
  //victorVD.writeMicroseconds(1100);
  //Serial.println("victorVD is turning left");
  //Serial.println(1500-turnSpeed);
}
if (curVal <= desVal && leftBump == 1) { //turn right
  additionalSpeed = (desVal - 0.5) * 700;
  turnSpeed = ((desVal - curVal) * 1000) + additionalSpeed;
  if (turnSpeed < 50) {
    turnSpeed = 50;
  }
  if (turnSpeed > 500) {
    turnSpeed = 500;
  }
  victorVD.writeMicroseconds(1500 + turnSpeed);
  //victorVD.writeMicroseconds(1900);
  //Serial.println("victorVD is turning right");
  //Serial.println(1500 + turnSpeed);
}
}

// Liam's Turn Equation
/*void turnCompute () {
  // Code to drive van door motor to desired position
  curVal = (potIn)/945; //set value of current pot position using range of 1000 to get % of turn
  desVal = (turnOut-1000)/1000; //set value of desired positon using % of turn
  //Serial.print("potIn is:");
  //Serial.println(potIn);
  //Serial.println("Pot Degree Val");
}

```

```

//Serial.println(potRadVal(potIn));

if ((curVal - .05) <= desVal && (curVal + .05) >= desVal) {
  victorVD.writeMicroseconds(fullStop);
  //Serial.println("victorVD is stopped:");
  //Serial.println(turnCh);
}
if (curVal >= desVal && rightBump == 1 ) { //turn left
  additionalSpeed = (0.5 - desVal) * 800;
  turnSpeed = ((curVal - desVal) * 1000) + additionalSpeed;
  if (turnSpeed < 50) {
    turnSpeed = 50;
  }
  if (turnSpeed > 500) {
    turnSpeed = 500;
  }
  victorVD.writeMicroseconds(1500 - turnSpeed);
  //victorVD.writeMicroseconds(1100);
  //Serial.println("victorVD is turning left");
  //Serial.println(1500-turnSpeed);
}
if (curVal <= desVal && leftBump == 1) { //turn right
  additionalSpeed = (desVal - 0.5) * 800;
  turnSpeed = ((desVal - curVal) * 1000) + additionalSpeed;
  if (turnSpeed < 50) {
    turnSpeed = 50;
  }
  if (turnSpeed > 500) {
    turnSpeed = 500;
  }
  victorVD.writeMicroseconds(1500 + turnSpeed);
  //victorVD.writeMicroseconds(1900);
  //Serial.println("victorVD is turning right");
  //Serial.println(1500 + turnSpeed);
}
}*/
// End

```

Appendix C: FRC Motor Data

	Character	Peak Power	At limit (W)	Free Speed (rpm)	Stall Torq	Allowed	On Hand
CIM	Robust/Heavy	340	275(40A)	5310	21.5	6	6+
MiniCIM	Robust/Heavy	205 (260?)	205 (40A)	6160	11.2	4*	
Bag Motor	Robust/Heavy	185 (168?)	180 (30A)	14000	4.4	"	
RS775-18	Sturdy/AC	270	265(40A)	13000	6.9	4*	
RS550-12	Smokeable/AC	250	245(40A)	19300	4.3	"	
RS550-12-B	"backshaft"	250	245(40A)	19300	4.3	"	
RS540-12		125	125 (20)	16800	2.5	"	
RS775-12	Sturdy/AC	83	80(20A)	7300	3.8	"	
RS545-12		75	75(10A)	16800	1.4	"	
RS395-12	Smokeable/AC	50	50(10A)	15500	1.0	"	
RS390-12		45	45 (10A)	12180	1.2	"	
Bosch Van Door	Robust	53	24.2 (20A)	48	360.0	2	
am-0912 (RS-500)	Smokeable/AC	180	150(20A)	16000	3.8	4	
am-2161 (RS 775-12?)						3*	
am-2194 (RS 775-12?)						"	
am-2235 (snow-)	Antibackdrive*	30	30 (20A)	100	100.0	1	1
Keyang (window)	Antibackdrive*	25	25(10A)	70	118.0	2*	
Denso (window)	Antibackdrive*	25	25(10A)	86	93.8	"	
Nippon-Denso (V)	Antibackdrive*	22	20(10A)	92	81.4	"	
Denso (throttle)	Sturdy*	18	18(5A)	5300	1.1	4	
VEX 393	Cute*	4	4 (2A)	100	14.8	2	2+

Appendix D: Power Requirement Data

Steer Angles	Linkage Angles	Coefficient of Friction	Max Weight (N)	Wheel Shaft Torque (Nm)	Linkage Shaft Torque (Nm)	Arm Force Needed (N)	Steer Arm Torque (Nm)	Arm Rotational Speed (rad/s)	Power Needed (W)
-19	10.25	0.65	533.786	4.406403	13.21921	88.14699	11.19467	0.785398	8.792271
-18	11.25	0.65	533.786	4.406403	13.21921	88.43957	11.23182	0.785398	8.821455
-17	12.25	0.65	533.786	4.406403	13.21921	88.76122	11.27267	0.785398	8.853538
-16	13.25	0.65	533.786	4.406403	13.21921	89.11246	11.31728	0.785398	8.888573
-15	14.25	0.65	533.786	4.406403	13.21921	89.49387	11.36572	0.785398	8.926617
-14	15.25	0.65	533.786	4.406403	13.21921	89.90606	11.41807	0.785398	8.967731
-13	16.25	0.65	533.786	4.406403	13.21921	90.34971	11.47441	0.785398	9.011983
-12	17.25	0.65	533.786	4.406403	13.21921	90.82556	11.53485	0.785398	9.059447
-11	18.25	0.65	533.786	4.406403	13.21921	91.33443	11.59947	0.785398	9.110204
-10	19.25	0.65	533.786	4.406403	13.21921	91.87717	11.6684	0.785398	9.16434
-9	20.25	0.65	533.786	4.406403	13.21921	92.45473	11.74175	0.785398	9.221949
-8	21.25	0.65	533.786	4.406403	13.21921	93.06813	11.81965	0.785398	9.283133
-7	22.25	0.65	533.786	4.406403	13.21921	93.71845	11.90224	0.785398	9.348
-6	23.25	0.65	533.786	4.406403	13.21921	94.40689	11.98968	0.785398	9.416669
-5	24.25	0.65	533.786	4.406403	13.21921	95.13472	12.08211	0.785398	9.489266
-4	25.25	0.65	533.786	4.406403	13.21921	95.90329	12.17972	0.785398	9.565928
-3	26.25	0.65	533.786	4.406403	13.21921	96.71408	12.28269	0.785398	9.646801

-2	27.25	0.65	533.786	4.406403	13.21921	97.56868	12.39122	0.785398	9.732043
-1	28.25	0.65	533.786	4.406403	13.21921	98.46877	12.50553	0.785398	9.821823
0	29.25	0.65	533.786	4.406403	13.21921	99.41619	12.62586	0.785398	9.916324
1	30.25	0.65	533.786	4.406403	13.21921	100.4129	12.75244	0.785398	10.01574
2	31.25	0.65	533.786	4.406403	13.21921	101.461	12.88555	0.785398	10.12029
3	32.25	0.65	533.786	4.406403	13.21921	102.5628	13.02548	0.785398	10.23019
4	33.25	0.65	533.786	4.406403	13.21921	103.7207	13.17253	0.785398	10.34568
5	34.25	0.65	533.786	4.406403	13.21921	104.9375	13.32706	0.785398	10.46705
6	35.25	0.65	533.786	4.406403	13.21921	106.2158	13.4894	0.785398	10.59455
7	36.25	0.65	533.786	4.406403	13.21921	107.5588	13.65997	0.785398	10.72851
8	37.25	0.65	533.786	4.406403	13.21921	108.9699	13.83917	0.785398	10.86926
9	38.25	0.65	533.786	4.406403	13.21921	110.4525	14.02747	0.785398	11.01715
10	39.25	0.65	533.786	4.406403	13.21921	112.0107	14.22535	0.785398	11.17257
11	40.25	0.65	533.786	4.406403	13.21921	113.6485	14.43336	0.785398	11.33593
12	41.25	0.65	533.786	4.406403	13.21921	115.3706	14.65207	0.785398	11.50771
13	42.25	0.65	533.786	4.406403	13.21921	117.182	14.88211	0.785398	11.68838
14	43.25	0.65	533.786	4.406403	13.21921	119.088	15.12417	0.785398	11.8785
15	44.25	0.65	533.786	4.406403	13.21921	121.0945	15.379	0.785398	12.07864
16	45.25	0.65	533.786	4.406403	13.21921	123.208	15.64741	0.785398	12.28945
17	46.25	0.65	533.786	4.406403	13.21921	125.4354	15.9303	0.785398	12.51163
18	47.25	0.65	533.786	4.406403	13.21921	127.7845	16.22863	0.785398	12.74594
19	48.25	0.65	533.786	4.406403	13.21921	130.2637	16.54349	0.785398	12.99323
20	49.25	0.65	533.786	4.406403	13.21921	132.8823	16.87605	0.785398	13.25442
21	50.25	0.65	533.786	4.406403	13.21921	135.6505	17.22761	0.785398	13.53054
22	51.25	0.65	533.786	4.406403	13.21921	138.5796	17.59961	0.785398	13.8227
23	52.25	0.65	533.786	4.406403	13.21921	141.6821	17.99363	0.785398	14.13216
24	53.25	0.65	533.786	4.406403	13.21921	144.9719	18.41143	0.785398	14.4603
25	54.25	0.65	533.786	4.406403	13.21921	148.4643	18.85497	0.785398	14.80866
26	55.25	0.65	533.786	4.406403	13.21921	152.1767	19.32644	0.785398	15.17895
27	56.25	0.65	533.786	4.406403	13.21921	156.1283	19.82829	0.785398	15.5731
28	57.25	0.65	533.786	4.406403	13.21921	160.3407	20.36327	0.785398	15.99327
29	58.25	0.65	533.786	4.406403	13.21921	164.8383	20.93447	0.785398	16.44189
30	59.25	0.65	533.786	4.406403	13.21921	169.6487	21.54539	0.785398	16.92171

Appendix E: Bosch Van Door Motor Output Data

Steer Angles	Linkage Angles	Steer Arm Force (N)	Tie Rod Force (N)	Linkage Shaft Torque (Nm)	Wheel Shaft Torque (Nm)
-19	10.25	498.38	490.4262	74.74095	24.91365
-18	11.25	498.38	488.8038	74.49369	24.83123
-17	12.25	498.38	487.0324	74.22374	24.74125
-16	13.25	498.38	485.1128	73.93118	24.64373
-15	14.25	498.38	483.0453	73.6161	24.5387
-14	15.25	498.38	480.8307	73.2786	24.4262
-13	16.25	498.38	478.4696	72.91877	24.30626

-12	17.25	498.38	475.9628	72.53674	24.17891
-11	18.25	498.38	473.3111	72.1326	24.0442
-10	19.25	498.38	470.5151	71.7065	23.90217
-9	20.25	498.38	467.5758	71.25855	23.75285
-8	21.25	498.38	464.4941	70.7889	23.5963
-7	22.25	498.38	461.2709	70.29768	23.43256
-6	23.25	498.38	457.9072	69.78505	23.26168
-5	24.25	498.38	454.404	69.25116	23.08372
-4	25.25	498.38	450.7624	68.69618	22.89873
-3	26.25	498.38	446.9834	68.12028	22.70676
-2	27.25	498.38	443.0684	67.52362	22.50787
-1	28.25	498.38	439.0183	66.90639	22.30213
0	29.25	498.38	434.8346	66.26879	22.0896
1	30.25	498.38	430.5183	65.61099	21.87033
2	31.25	498.38	426.071	64.93322	21.64441
3	32.25	498.38	421.4938	64.23566	21.41189
4	33.25	498.38	416.7883	63.51854	21.17285
5	34.25	498.38	411.9558	62.78206	20.92735
6	35.25	498.38	406.9978	62.02647	20.67549
7	36.25	498.38	401.9159	61.25198	20.41733
8	37.25	498.38	396.7115	60.45883	20.15294
9	38.25	498.38	391.3863	59.64726	19.88242
10	39.25	498.38	385.9418	58.81753	19.60584
11	40.25	498.38	380.3798	57.96988	19.32329
12	41.25	498.38	374.7019	57.10457	19.03486
13	42.25	498.38	368.9099	56.22187	18.74062
14	43.25	498.38	363.0055	55.32204	18.44068
15	44.25	498.38	356.9906	54.40536	18.13512
16	45.25	498.38	350.8669	53.47211	17.82404
17	46.25	498.38	344.6363	52.52257	17.50752
18	47.25	498.38	338.3007	51.55703	17.18568
19	48.25	498.38	331.8621	50.57578	16.85859
20	49.25	498.38	325.3224	49.57913	16.52638
21	50.25	498.38	318.6836	48.56738	16.18913
22	51.25	498.38	311.9477	47.54084	15.84695
23	52.25	498.38	305.1168	46.49981	15.49994
24	53.25	498.38	298.193	45.44462	15.14821
25	54.25	498.38	291.1783	44.37558	14.79186
26	55.25	498.38	284.075	43.29303	14.43101
27	56.25	498.38	276.8851	42.19729	14.06576
28	57.25	498.38	269.6109	41.08869	13.69623
29	58.25	498.38	262.2545	39.96759	13.32253
30	59.25	498.38	254.8182	38.8343	12.94477